Universidade de Aveiro

Secção Autónoma de Ciências da Saúde

2011

Joana Vieira da Silva

Electron microscopy study of PP1 and SARP2 in human testis

Estudo por microscopia electrónica da PP1 e SARP2 em testículo humano

Universidade de Aveiro

Secção Autónoma de Ciências da Saúde

2011

Joana Vieira da Silva

Electron microscopy study of PP1 and SARP2 in human testis

Estudo por microscopia electrónica da PP1 e SARP2 em testículo humano

Dissertação apresentada à Universidade de Aveiro para cumprimento dos requisitos necessários à obtenção do grau de Mestre em Biomedicina Molecular, realizada sob a orientação científica da Doutora Margarida Sâncio da Cruz Fardilha, Professora auxiliar convidada da Secção Autónoma de Ciências da Saúde da Universidade de Aveiro e co-orientação da Doutora Odete Abreu Beirão da Cruz e Silva, Professora auxiliar da Secção Autónoma de Ciências da Saúde da Universidade de Aveiro.

Dedico este trabalho ao meu avô.

o júri

presidente

Prof. Doutora Liliana Xavier Marques de Sousa
Professora auxiliar com agregação da Secção Autónoma de Ciências da Saúde da Universidade de Aveiro

Prof. Doutora Odete Abreu Beirão da Cruz e Silva
Professora auxiliar com agregação da Secção Autónoma de Ciências da Saúde da Universidade de Aveiro

Prof. Doutor Georg Luers
Professor do Hospital Universitário Hamburg-Eppendorf

Prof. Doutora Margarida Sâncio da Cruz Fardilha
Professora auxiliar convidada da Secção Autónoma de Ciências da Saúde da Universidade de Aveiro

agradecimentos

Á Prof. Margarida Fardilha, porque a ela devo a maior parte dos conhecimentos que tenho; por me ensinar a ser optimista, paciente e esperar sempre o melhor; por ser um exemplo de que é possível conciliar ciência e família.

To Prof. Georg Luers. I truly appreciate his hospitality, patience and sympathy. He taught me to think critically and to pay attention to details.

Á Prof. Odete da Cruz e Silva pela força e incentivo.

Ao Centro de Biologia Celular e CRUP, acção integrada nº A-14/10.

A todos os meus colegas do CBC pelos bons momentos, pelo apoio, discussão de ideias, paciência e boa disposição que tornaram este trabalho muito mais fácil. Em especial ao Korrodi e à Sara.

Ao Hélder e ao Paulo que se mantêm presentes ao fim de tantos anos.

Aos amigos que fiz durante a universidade, que tornaram estes últimos 5 anos, os melhores da minha vida. Em especial à Guida, Oliveira, Rocha, Edgar e Igor.

Ao Miguel.

Aos meus avós e padrinhos pelo apoio e confiança incondicionais.

Aos meus pais por serem um verdadeiro exemplo de felicidade, compreensão e dedicação; porque a eles devo grande parte daquilo que sou.

palavras-chave

fosforilação de proteínas, proteína fosfatase 1, SARP2, testículo humano, epidídimo humano, microscopia electónica

resumo

A proteína fosfatase-1 (PP1) é uma fosfatase específica para a desfosforilação de resíduos de serina e treonina, cujas funções celulares dependem da formação de complexos com proteínas que interagem com a PP1 (PIPs). Dada a importância da PP1γ2, isoforma específica de testículo/espermatozóides, na espermatogénese e na função dos espermatozóides, é fundamental identificar as funções das PIPs específicas destes tecidos, tais como a SARP2 (Several Ankyrin Repeat Protein 2). A PP1 alcança a sua especificidade, não só pela diversidade de proteínas com as quais interage, mas também através de diferentes subunidades catalíticas. No entanto, a maioria dos estudos não aborda directamente a importância das diferentes isoformas da PP1.

Neste trabalho relatamos, pela primeira vez, os padrões de expressão de PP1γ2, PP1α e SARP2 no testículo humano, colhido in vivo, por microscopia electrónica. Os nossos resultados demostram que a PP1γ2 é a isoforma mais abundante nos estágios finais de maturação das células germinativas masculinas, enquanto que a PP1α está presente no núcleo dos espermatídeos e durante a formação do acrossoma. A SARP2 é altamente abundante no testículo no qual é expressa apenas na fase pós-meiótica, mais especificamente na fase média/tardia dos espermatídeos haplóides elongados. Dado este padrão de localização de SARP2, propomos que esta possa desempenhar um papel importante na diferenciação e/ou função dos espermatozóides.

Em conclusão, a SARP2 e a PP1γ2, proteínas abundantes em testículo e espermatozóides, apresentam a mesma localização no testículo humano. O complexo PP1γ2/SARP2 revela especificidade a nível tecidular (testículo), de estadío de espermatogénese (espermiogénese), a nível celular (espermatídeos elongados) e da localização sub-celular (núcleo), o que torna o complexo um novo alvo para a contracepção masculina ou tratamento de infertilidade masculina.

keywords

protein phosphorylation, protein phosphatase 1, SARP2, human testis, human epididymis, electron microscopy

abstract

Protein Phosphatase 1 (PP1) is a major eukaryotic serine/threonine specific phosphatase whose cellular functions depend on the complexes it forms with PP1 Interacting Proteins (PIPs). Given the importance of the testis/sperm-enriched variant, PP1γ2, in spermatogenesis and sperm function it is imperative to identify the roles of the testis/sperm specific PIPs, such as SARP2 (several ankyrin repeat protein 2). PP1 achieves its specificity towards the substrates not only by the diversity of the binding partners but also through different catalytic subunits. Most studies have not directly addressed the significance of the different isoforms.

Here, we report, for the first time, the expression patterns of PP1α, PP1γ2 and SARP2 in human testis by immunoelectron microscopy, using tissue previously collected *in vivo*. Our results show that PP1γ2 is the most abundant isoform in the late stages of germ cell maturation, whereas for the most part, PP1α is found in spermatids nucleus and during the acrosome formation. SARP2 exhibits a tissue, cell type, and spermatogenic stage specificity. SARP2 is more abundant in testis, and within the testis it is expressed only in post-meiotic haploid spermatids, mainly in mid/late stages of elongated spermatids. Given this unique expression pattern of SARP2, we propose that it plays a significant role in sperm differentiation and/or function.

In conclusion, SARP2 shows the same localization pattern in human testis as PP1γ2, the PP1 testis/sperm-specific isoform. PP1γ2/SARP2 complex is tissue (testis), spermatogenic stage (spermiogenesis), cell type (elongated spermatids) and subcellular compartment (nucleus) specific. Thus making this complex a putative novel target for male contraception or male infertility treatment.

ABBREVIATIONS **1**

1. INTRODUCTION **5**

1.1. Overview on the Male Reproductive System 7

1.1.1. Testis 7

1.1.1.1. The Testicular Seminiferous Tubules 8

1.1.1.1.1. Peritubular Myoid Cells – The Contraction Cells 8

1.1.1.1.2. Sertoli Cells – The Supporting Cells 8

1.1.1.2. Leydig Cells – The Interstitial Cells 8

1.1.2. Spermatogenesis 9

1.1.3. The Cycle of the Seminiferous Epithelium 10

1.1.4. Genital Ducts 11

1.1.4.1. Epididymis 11

1.2. Protein Phosphorylation and Protein Phosphatases 13

1.3. Protein Phosphatase 1 14

1.3.1. PP1 Catalytic Subunit 14

1.3.2. PP1 Interacting Proteins 16

1.3.3. PP1 Distribution and Expression 21

1.3.4. PP1 and Testis Function 22

1.3.4.1. Testis/Sperm-Specific PIPs 23

1.3.4.2. Alternative Splicing in Testis 24

1.3.5. SARP – A PP1 interacting protein 24

1.4. Aims 26

2. ULTRASTRUCTURE ANALYSES OF THE HUMAN TESTIS AND EPIDIDYMIS **27**

2.1. Material and Methods 29

2.1.1. Human Samples Collection 29

2.1.2. Electron Microscopy 29

2.1.2.1. Fixation and Post-Fixation 29

2.1.2.2. Dehydration and Embedding 30
2.1.2.3. Sectioning, Contrast Staining and Observation 30
2.2. Results 32
2.2.1. Testis Semi-Thin Sections and Ultra-Thin Sections 32
2.2.2. Electron Microscopy Analyses of Human Testis 33
2.2.2.1. Testis Overview 33
2.2.2.2. Basal Compartment 34
2.2.2.3. Sertoli Cell 35
2.2.2.4. Leydig Cell 36
2.2.2.5. Spermiogenesis 36
2.2.3. Electron Microscopy Analyses of the Human Epididymis 38
2.3. Discussion 40
2.3.1. Human Testis 41
2.3.2. Human epididymis 42

3. LOCALIZATION OF PP1 ISOFORMS AND SARP2 ON HUMAN TESTIS 45

3.1. Material and Methods 47
3.1.1. Antibodies 47
3.1.2. Human Samples Collection 48
3.1.3. Western Blot Analyses 48
3.1.3.1. Tissues Preparation 48
3.1.3.2. Calculate the Concentration and the Total Number of Spermatozoa in Semen Sample 49
3.1.3.3. SDS-PAGE 49
3.1.3.4. Immunoblotting 50
3.1.4. Immunoelectron Microscopy 51
3.1.5. Immunohistochemistry 53
3.2. Results 54
3.2.1. Specificity of SARP2 Antibody in Human Testis 54
3.2.2. Localization of PP1 Isoforms and SARP2 in Human Testis 54

3.2.2.1. Localization of PP1 Isoforms in Human Testis by IEM 55

3.2.2.2. Localization of SARP2 in Human Testis 58

3.2.3. Localization of PP1 Isoforms and SARP2 in Human Testis Immunohistochemistry 59

3.2.3.1. PP1 Isoforms 59

3.2.3.2. SARP2 60

3.3. Discussion 61

3.3.1.1. PP1 Isoforms in human testis 63

3.3.1.2. SARP2 in Human Testis 64

4. FINAL CONCLUSIONS 67

REFERENCES 71

APPENDIX 83

ABBREVIATIONS

5' RACE	5 prime rapid amplification of cDNA end
Aa	Amino acid
AC	Adenylyl cyclase
ADP	Adenosine diphosphate
ATP	Adenosine triphosphate
AKAP	A-kinase-anchoring protein
APS	Ammonium persulfate
Bmp	Bone morphogenetic protein
BRCA1	Breast cancer 1
Ca^{2+}	Calcium
cAMP	Cyclic AMP (Adenosine 3´, 5´-monophosphate)
cDNA	complementary deoxyribonucleic acid
CPI-17	Protein kinase C potentiated inhibitor
Da	Dalton
DARPP-32	Dopamine and cAMP-regulated phosphoprotein 32 kDa
DNA	Deoxyribonucleic acid
FCP	TFIIF-associating C-terminal domain phosphatases
GADD34	Growth Arrest and DNA Damage-Inducible Protein
GM	Glycogen-targeting subunit
GSK-3	Glycogen synthase kinase 3
hCG	Human chorionic gonadotrophin
Hox11	Homeobox 11
Hr	Hour
I-1	Inhibitor-1
I-2	Inhibitor-2
I-3	Inhibitor-3
IGF-I	Insulin-like growth factor 1
IRBIT	Inositol 1,4,5-trisphosphate receptor-binding protein
LB	Loading buffer
LH	Luteinizing hormone
LGB	Lower gel buffer
min	Minute
mRNA	Messenger ribonucleic acid

MAPK	Mitogen-activated protein kinase
MYPT	Myosin phosphatase targeting subunit
Nek2	NimA-related protein kinase
NIPP1	Nuclear inhibitor of protein phosphatase 1
NO	Nitric oxide
NOM1	Nucleolar protein with MIF4G domain 1
ON	Overnight
PER2	Period circadian protein homolog 2
PI3	Phosphatidyl inositol kinase-3
PIPs	PP1-interacting proteins
PIP2	Phosphatidylinositol 4,5-bisphosphate
PITK	Phosphatase Interactor Targeting K protein
PNUTS	Protein Phosphatase 1 Nuclear Targeting Subunit
PP1-7	Protein phosphatase 1-7
PP1c	Protein phosphatase 1 catalytic subunit
PPM	Metal ion dependent protein phosphatase
PPP	Phosphoprotein phosphatase
Pro	Proline
PRIP	Phospholipase C-related inactive protein
PTP	Protein tyrosine phosphatase
RIPP1	Ribosomal inhibitor of PP1
ROS	Reactive Oxygen Species
RNA	Ribonucleic acid
RT	Room temperature
SDS	Sodium dodecyl sulphate
SARA	SMAD anchor for receptor activation
SCP	Small C-terminal domain phosphatase
sec	seconds
Ser	Serine
sER	Smooth endoplasmic reticulum
STPPs	Serine/threonine protein phosphatases
TAT-1	Transactivating regulatory protein 1
TBS	Tris-buffered saline
TBST	TBS supplemented with Tween-20 detergent
TEMED	N, N, N´, N' – Tetramethylethylenediamine

TIMAP	Transforming growth factor β inhibited, membrane-associated protein
TGFβ	Transforming growth factor beta
Thr	Threonine
TLRR	Testis leucine-rich repeat
Tyr	Tyrosine
YTH	Yeast two-hybrid
UGB	Upper gel buffer

1. INTRODUCTION

1.1. OVERVIEW ON THE MALE REPRODUCTIVE SYSTEM

The male reproductive system consists of two testes, a system of genital ducts, the accessory glands and the penis. This system functions in the formation of spermatozoa (spermatogenesis), the production of male sex hormones (steroidogenesis) and the delivery of male gametes into female reproductive tract (Standring, 2005).

1.1.1. TESTIS

Testes are oval structures housed in a separate compartment within the scrotum (Standring, 2005). Each human testis contains hundreds of tightly packed seminiferous tubules, ranging from 150 to 250 µm in diameter and from 30 to 70 cm long. Each highly convoluted seminiferous tubule is composed of a fibromuscular tunica propria, which is separated from the seminiferous epithelium by a basal membrane (Figure 1). The seminiferous epiphelium is composed of sustentacular Sertoli cells and a stratified layer of developing male germ cells (Figure 1, B). Sertoli cells establish a blood-barrier by forming tight junctions with each other, thus dividing the seminiferous tubule into basal and adluminal compartments (Figure 1,C).

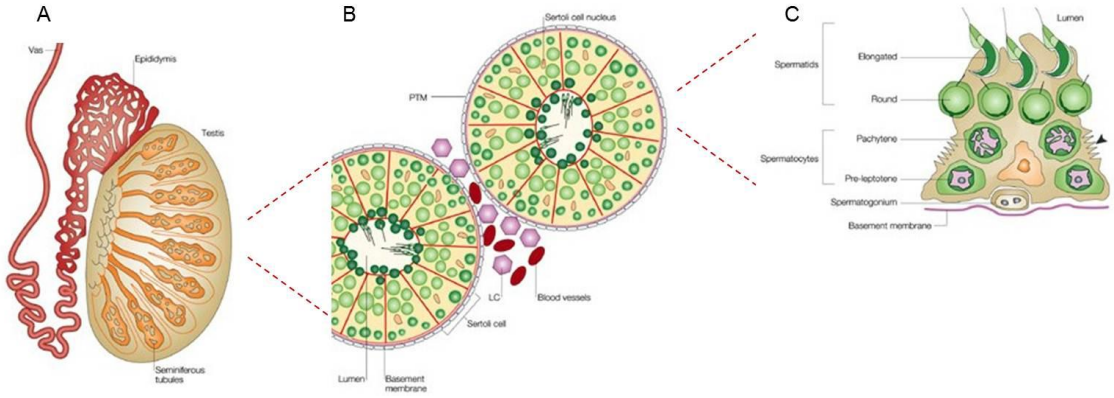

Figure 1| Human Testis. A| Cross-section through a testis, showing the seminiferous tubules, the epididymis and the *vas deferens* B| A diagrammatic cross-section through a testicular tubule, showing the germ cells (green) at different stages of maturation embedded in somatic Sertoli cells (each Sertoli cell is outlined in red). Leydig cells (LC) are present in the interstitium. Maturing sperm are shown in the lumen of the tubules. PTM, peritubular myoid cell. C| A Sertoli cell with its associated germ cells. Note that tight juctions between Sertoli cells (arrowhead) define two compartments: the stem cells and the pre-meiotic cells (spermatogonia) are found on one side of the junction, whereas the meiotic (spermatocytes) and the post-meiotic (round and elongating spermatids) cells are found organized in strict order of maturation towards the lumen (cytoplasm is shown in dark green, DNA is shown in pink, Sertoli cell nucleus is shown in orange). Adapted from (Cooke *et al.*, 2002).

1.1.1.1. THE TESTICULAR SEMINIFEROUS TUBULES

1.1.1.1.1. PERITUBULAR MYOID CELLS – THE CONTRACTION CELLS

Several layers of peritubular myoid cells exist in the tunica propria of the seminiferous tubules (Figure 1, B). These cells are joined by junctional complexes. These cellular layers are responsible for the irregular contractions of the seminiferous tubules which propel fluid secreted by the Sertoli cells, together with testicular spermatozoa into the lumen and through the tubular network (Ross *et al.*, 1966). Several substances (TGFβ, prostaglandins, oxytocin, NO) have been suggested to affect the contraction of this cell type. Peritubular myoid cells also participate in the regulation of processes within the seminiferous tubules by the production of growth factors (e.g. PModS, activin, IGF-I) and extracellular matrix components (fibronectin, type I and IV collagens) (Maekawa *et al.*, 1996).

1.1.1.1.2. SERTOLI CELLS – THE SUPPORTING CELLS

Sertoli cells provide the structural organization of the seminiferous tubules (Clermont *et al.*, 1957) (Figure 1, C). These cells do not replicate after puberty and their number determines the testicular size, germ cell numbers and spermatozoa output (Orth *et al.*, 1988; Larry *et al.*, 2008). Sertoli cells are involved in (1) maintenance of the integrity of the seminiferous epithelium by establishing the blood-testis barrier, (2) mechanical support and nutrition of germ cells, (3) paracrine regulation of male germ cell proliferation and differentiation by secretion of regulatory proteins, including peptide growth factors and hormones, (4) phagocytosis, (5) steroid hormone synthesis and metabolism (Larry *et al.*, 2008).

1.1.1.2. LEYDIG CELLS – THE INTERSTITIAL CELLS

Leydig cells lie within the intertubular region of the testis and are found adjacent to the blood vessels, reflecting their endocrine function (Figure 1, B). They are the cell type responsible for testosterone production, which is essential for maintenance of spermatogenesis. In most species there are two generations of Leydig cells (Gould *et al.*, 1979; Lejeune *et al.*, 1998; Svechnikov *et al.*, 2010). A fetal generation under the stimulation of human Chorionic Gonadotropin (hCG) results in the production of testosterone during gestation in humans, but these cells decrease in number and are lost from the intertubular space around twelve months of age (Prince, 1990). The adult generation of Leydig cells in humans results from Luteinizing Hormone (LH) stimulation starting at puberty (Christensen *et al.*, 1980; Benton *et al.*, 1995).

1.1.2. SPERMATOGENESIS

The duration of the entire process of spermatogenesis varies between species, for example, 35 days in the mouse and hamster, 50 days in the rat, 45 to 65 days in various nonhuman primates, and 70 days in humans (Figure 2) (de-Kretser *et al.*, 1994). In humans, release of spermatozoa occurs in the early stages of puberty at approximately 13.5 years of age, and spermatogenesis continues throughout life. The quantitative output of spermatozoa in an adult man is remarkable and equivalent to approximately 1000 new sperm per second (de-Kretser *et al.*, 1994).

Spermatogenesis can be divided into three major phases: (1) proliferation and differentiation of spermatogonia, (2) meiosis and (3) spermiogenesis and spermiation (Figure 2) (McLachlan *et al.*, 2002; Yoshida *et al.*, 2007).

In human testes, essentially three types of spermatogonia are recognized (A dark, A pale, and B), but additional types of A spermatogonia have been suggested by electron microscopy (Aponte *et al.*, 2005; Ehmcke *et al.*, 2006a; Ehmcke *et al.*, 2006b). Classification of these cells is based on features of their nuclei and, in particular, their chromatin patterns. Spermatogonia proliferation and differentiation involves renewal of progenitor A dark and A pale spermatogonia, division of commited A pale spermatogonia to form type B, and their division to form preleptotene spermatocytes (Hermo *et al.*, 2010).

Cells undergoing meiosis are primary spermatocytes, in which the preleptotene stage is characterized by DNA synthesis. Chromosome number remains diploid but DNA content doubles. Leptotene spermatocytes begin in prophase, and then gradually enter the zygotene phase when homologous chromosomes pair and synapse. Cells continue to increase in volume until the pachytene stage of premeiotic chromosomal recombination. The subsequent first meiotic division produces secondary spermatocytes, in which chromosome number is halved, thereby defining haploidy, and DNA content per cell is reduced from 4N to 2N. Secondary spermatocytes then undergoe the second meiotic division without an intervening S phase of DNA synthesis to form 1N spermatids.

Spermiogenesis, the transformation of conventional round spermatids into spermatozoa includes a complex sequence of events: (a) formation of the acrosome, (b) condensation of the nucleus, (c) development of the tail, (d) reorganization of cellular organelles such as centrioles and mitochondria, (e) reduction of the cytoplasm, and (f) the process of release from the Sertoli cell, termed spermiation. All these events are associated with extensive changes in cell shape and size, and germ cell movement. The cytoskeleton is believed to function in these cellular events (Lie *et al.*, 2010). However, few studies have been conducted to unravel the role of the cytoskeleton during spermatogenesis.

1.1.3. THE CYCLE OF THE SEMINIFEROUS EPITHELIUM

Within the seminiferous epithelium, the cell types that constitute the process of spermatogenesis are highly organized to form a series of cell stages (Amann, 2008). LeBlond and Clermont defined the cycle of the seminiferous epithelium as all series of changes in a given area of the tubule between two appearances of the same development stages (LeBlond *et al.*, 1952). The human spermatogenesis can be divided into 6 stages (Figure 2). However, each stage often only occupy one quadrant of a tubule giving a disorganized appearance (Figure 3) (Clermont, 1963). The progression of each cell type in spermatogenesis involved a defined duration. The duration of a cycle in humans takes 16 days and the progression from spermatogonia to spermiation, resulting in spermatozoa, takes approximately 74 days (Figure 2) (Clermont, 1963; Heller *et al.*, 1964).

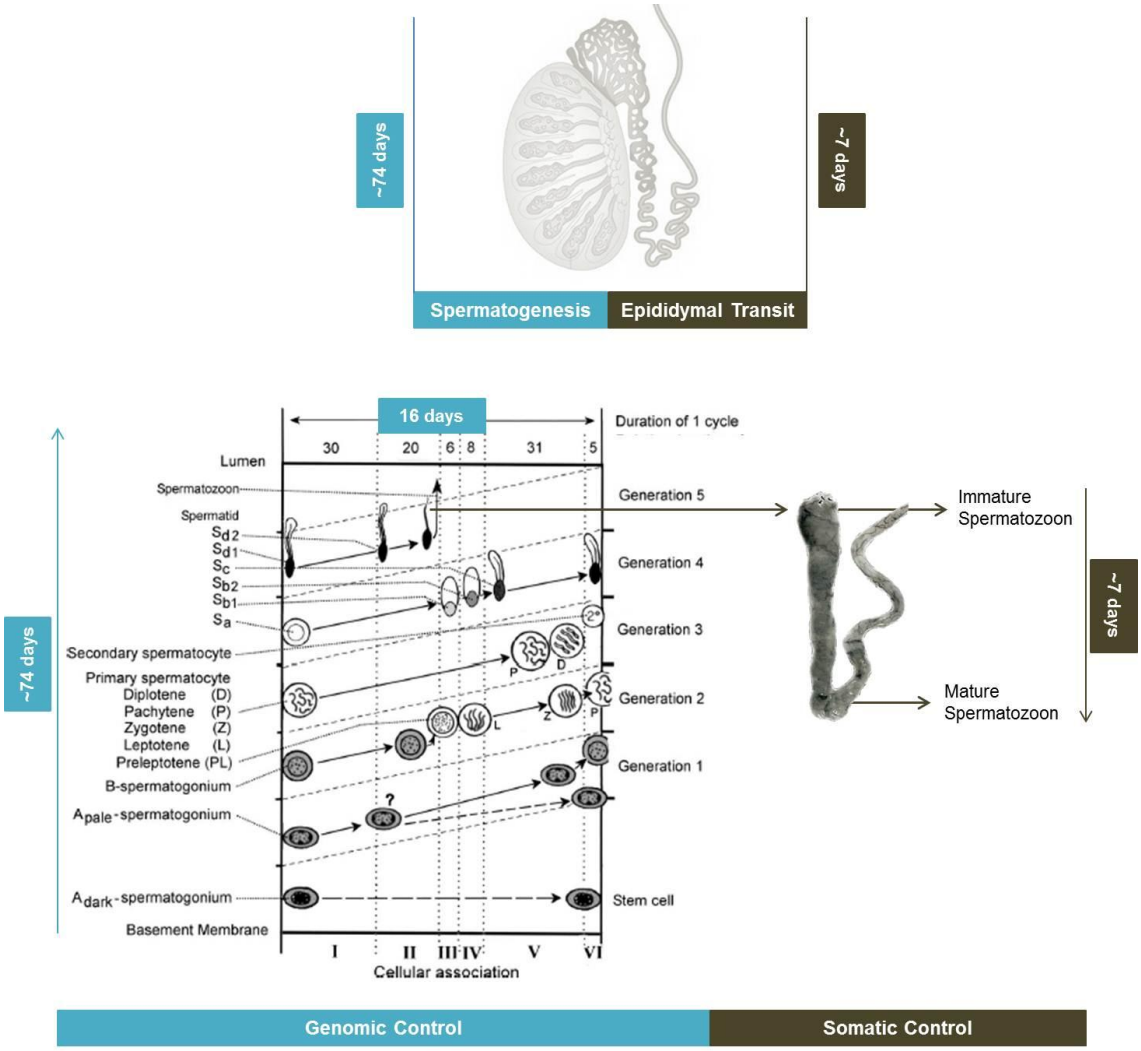

Figure 2| Human spermatogenesis (left) and sperm maturation (right). On the left, in the x axis are the 6 cellular associations on human testis. The types of germ cells present in each cellular association are on the axis of y (upward from the basement membrane to the lumen). In humans, the interval between commitment

of an A pale spermatogonia to spermatozoa averages 74 days. On the right, a series of sequential interactions with the epididymal fluid are believed to induce the final steps of sperm maturation. The time estimate for sperm to migrate through the human epididymis varies from a mean of 7-10 days (Rowley et al., 1970). Faster transit (up to 2 days) was estimated for men with large daily sperm production (Johnson et al., 1988).

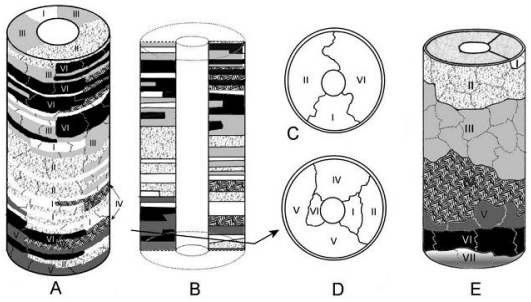

Figure 3| Diagrams of cellular associations in a portion of a human seminiferous tubule (A-D) and a seminiferous tubule from an animal such as bull, mouse, rabbit or rat (E) (Amann, 1981).

1.1.4. GENITAL DUCTS

A system of genital ducts conveys the spermatozoa and the fluid that composes semen to the outside. The seminiferous tubules are connected by short straight tubules, the *tubuli recti*, to the rete testis, which is composed of labyrinthine spaces located in the mediastinum testis. From here, spermatozoa enter the first part of the epididymis, the *ductuli efferentes* that lead into the *ductus epididymis*. Spermatozoa then enters in the *vas deferens*, a muscular structure that passes through the inguinal canal, as a part of the spermatic cord, to gain access to the abdominal cavity. The seminal vesicle empties its secretions into the *vas deferens*, which terminates at this point. The continuation of the duct, known as ejaculatory duct, enters the prostatic gland, which delivers its secretory product. Both ejaculatory duct (right and left) empty into the urethra, which conveys semen to the outside (Standring, 2005).

1.1.4.1. EPIDIDYMIS

The human epididymis is a long convoluted tubule that serves as a conduit for the transport of spermatozoa from the testis to the *vas deferens* and is the site where spermatozoa mature and acquire their functions of progressive motility and fertility (Figure 4) (Olson *et al.*, 2002). Additionally the epididymis plays functions in: reabsorption of fluid from seminiferous tubules, elimination of defective male gametes, and sperm protection against oxidative damage (Vernet *et al.*, 2004).

Epididymal sperm maturation involves a series of modifications: (1) remodelling of the sperm plasma membrane, (2) changes in composition and cellular localization of the proteins, (3) alteration of the glycoproteins content and (4) changes in pH and in the levels of Ca^{2+} and cAMP (Vijayaraghavan *et al.*, 1986, Bedford, 1990 #318; Huang *et al.*, 2004). Unfortunately, very little is known about the human epididymis and its role in sperm maturation owing to the lack of studies that have used normal human tissue from healthy men at reproductive age. Sperm maturation involves the interaction with proteins that are synthesized and secreted in a region-dependent manner from the epididymal epithelium (Figure 2). To understand the molecular mechanisms that are required for epididymal sperm maturation it is important to access the ultrastructure characteristics of the epithelial cells and their specific secretory activity according to the epididymal region. As stated in several epididymal protein, mRNAs and gene profiling studies it is possible that major differences in secretory activity of the human epididymis are confined to the most proximal region (*caput*) which consists of efferent ducts of varying epithelia (Zhang *et al.*, 2006); (Dubé *et al.*, 2007; Thimon *et al.*, 2007).

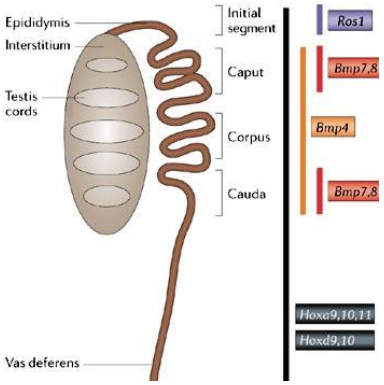

Figure 4| The epididymis can be divided, morphologically and functionally into *caput, corpus* and *cauda*. The sperm mature during their passage through the *caput* and *corpus*, whereas the *cauda* functions predominantly for storage. The different segments of the male genital tract are marked by specific gene expression. Null mutations of these genes result in phenotypes that are restricted to these segments. In Hoxa10 null mice the cauda seems to be transformed in the corpus, whereas in Hoxa11 knockout mice the vas deferens shows partial transformation in cauda. Mutations in bone morphogenetic protein 4 (Bmp4) result in extensive degeneration of the epididymal epithelium of the corpus region, rather than in the caput and cauda regions as for Bmp7 and Bmp8 knockout mice, whereas mice that are null for Ros1 show defects in the differentiation of the initial segment. Adapted from (Wilhelm *et al.*, 2006).

The importance of understanding epididymal sperm maturation is emphasized by the fact that up to 40% of infertile man exhibit idiopathic infertility that may reflect sperm maturational disorders. Other important aspect is the potential to identify epididymal mechanisms that could serve as targets for non-steroidal-based male contraceptives (Hinton *et al.*, 2010).

1.2. PROTEIN PHOSPHORYLATION AND PROTEIN PHOSPHATASES

Reversible protein phosphorylation represents one of the most common post-translational modification and plays a major role in cell viability with both protein kinases and phosphatases participating in this process by respectively adding or removing a phosphate group in the target substrates (Figure 5) (Fardilha *et al*, 2010).

Phosphorylation is a reaction where a phosphate group is added through a phosphoester bond (O-phosphate) to the hydroxyl side chain of different amino acid residues such as: Serine (Ser), Threonine (Thr) and Tyrosine (Tyr), with each accounting for approximately 86%, 12% and 18% of the human phosphoproteome (Olsen *et al*., 2006). The phosphate group may also be added to other residues such aspartate, histidine and arginine or to specific lipids such as PIP2.

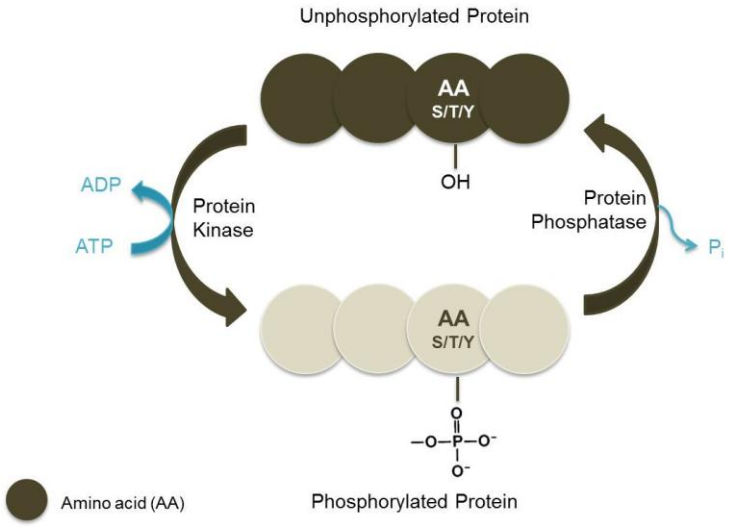

Figure 5| Protein phosphorylation/dephosphorylation mechanism. Kinases transfer a phosphate group from an ATP molecule to the hydroxyl side chain of the target amino acid, while phosphatases remove the phosphate group from the protein.

Protein phosphatases (PPs) can be divided in serine/threonine protein phosphatases (STPPs), tyrosine phosphatases and the dual specific phosphatases that dephosphorylate all three residues. Sequencing of entire genomes has revealed that approximately 3% of all eukaryotic genes encode kinases or PPs. Surprisingly, there appear to be 2-5 times fewer PPs than kinases, but at the holoenzyme level, the numbers of Ser/Thr specific protein kinases and phosphatases are roughly balanced. The diversity of Ser/Thr-specific PPs (STPPs) was achieved not only by the catalytic subunits, but also by the ability of a single catalytic subunit to interact with multiple interacting proteins (for review see Fardilha *et al*, 2010).

STPPs comprise three distinct gene families: the PPM (Mg^{2+} or Mn^{2+} dependent protein phosphatases), the FCP (TFIIF-associating C-terminal domain phosphatases) and the PPP (phosphoprotein phosphatases). The PPM family comprises the Mg^{2+}-dependent PPs, such as pyruvate dehydrogenase, PP2C, and relatives (Barford *et al.*, 1998). The FCP family comprises FCP1 and SCPs 1-3 PPs (Gallego *et al.*, 2005). Finally the PPP family includes PP1, PP2A, PP4, PP6, PP2B, PP5 and PP7 gene subfamilies that share high homology in catalytic domains but differ in the N- and C-terminal (Cohen, 1997; Barford *et al.*, 1998).

1.3. PROTEIN PHOSPHATASE 1

1.3.1. PP1 CATALYTIC SUBUNIT

PP1 is a major STPP involved in a wide range of cellular processes such as cell cycle progression, protein synthesis, muscle contraction, glycogen metabolism, cytokinesis, and neuronal signalling (Figure 6) (Cohen, 2002; Ceulemans *et al.*, 2004).

PP1 holoenzymes are composed of a highly conserved catalytic subunit termed Protein Phosphatase 1 catalytic subunit (PP1c) and one or two regulatory subunits known as PP1 Interacting Proteins (PIPs) (Bollen *et al.*, 2010). Eukaryotic genomes contain somewhere between one (*Saccharomyces cerevisiae*) and eight (*Arabidopsis thaliana*) genes that encode PP1c isoforms. In mammals, PP1c is encoded by three separate genes (*Ppp1ca*, *Ppp1cb* and *Ppp1cc*), each one of them suffering alternative splicing contributing to PP1 holoenzyme diversity (Shima *et al.*, 1993). The *Ppp1cc* gene, in particular, undergoes tissue-specific splicing, giving rise to a ubiquitously expressed isoform, PP1γ1, and a testis-enriched and sperm specific isoform, PP1γ2. The strictly difference between these different isoforms resides mainly in the carboxyl-terminus (da Cruz e Silva *et al.*, 1995). The same PP1 isoform, depending on the regulatory subunit that it is interacting with, may be in different subcellular compartments, fulfilling different functions.

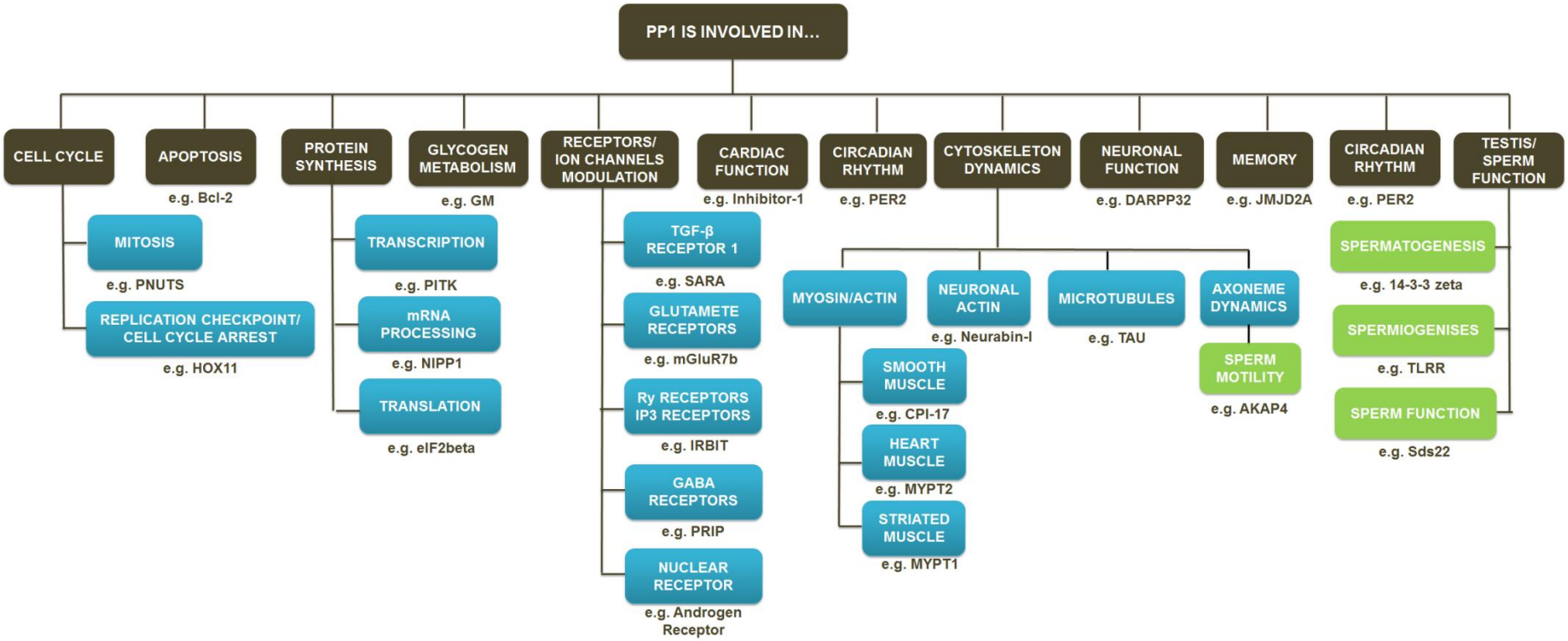

Figure 6| Schematic representation of PP1 functions. For each function, a PIP, whose interaction is relevant and well documented, is indicated. Testis/sperm specific functions are enhanced in green.

PNUTS (Landsverk et al., 2005); Hox11 (Kawabe et al., 1997); Bcl-2 (Ayllón *et al.*, 2001); PITK (Kwiek et al., 2006); NIPP1 (Trinkle-Mulcahy et al., 1999); eIF2beta (Wakula et al., 2006); GM (Toole *et al.*, 2007); SARA (Bennett *et al.*, 2002); mGluR7b (Enz, 2002); IRBIT (Ando et al., 2006); PRIP ; Androgen Receptor (Chen *et al.*, 2009); Inhibitor-1 (Nicolaou *et al.*, 2009) ;CPI-17 (Eto, 2009); MYPT2 ; MYPT1 (Terrak et al., 2004); Neurabin-I (MacMillan et al., 1999); TAU (Sobue et al., 2000); AKAP4 (Huang et al., 2005); DARPP32 (Svenningsson *et al.*, 2004); JMJD2A (Koshibu et al., 2009); PER2 (Gallego et al., 2006); 14-3-3 (Margolis et al., 2003); TLRR (Wang *et al.*, 2010); Sds22 (Mishra *et al.*, 2003).

1.3.2. PP1 INTERACTING PROTEINS

In the last two decades it has become clear that the more than two hundred PIPs found to date confer the specificity to PP1c by targeting it to a specific subcellular compartment, modulating its specificity or serving as substrates (Andreassen *et al.*, 1998; Barford *et al.*, 1998; Trinkle-Mulcahy *et al.*, 2001; Terry-Lorenzo *et al.*, 2002; Bollen *et al.*, 2010; Fardilha *et al.*, 2010). The key to understand the function of PP1 lies in identifying and studying the subcellular roles of the PIPs.

PIPs are structurally unrelated, but most of them share a short, degenerate RVXF-type docking motif that binds to a hydrophobic groove located on a surface behind the PP1c active site (Table 1) (Hendrickx *et al.*, 2009). Other PP1 binding motifs, beyond RVxF, are shown in Table 1.

Table 1| PP1 binding motifs. Further than RVxF, there are other PP1 binding motifs such as, SILK and MyphoNE motifs. Examples for PIPs with other motifs beyond RVxF are also shown. aa, amino acid;

RVxF motif **(N- and C-terminal of the motif should have 4 or 5 basic (KR) and acidic (DE) aa)**		
[RK]-X(0,1)-[VI]-{P}-[FW] X(0,1) is any aa, present or absent**;** {P} represents any aa except P		Wakula et al. 2003
[HKR]-[ACHKMNQRSTV]-V-[CHKNQRST]-[FW]		Meiselbach et al. 2006
$[K_{54}R_{34}L_4]$-$[K_{28}R_{26}S_{10}T_9A_8M_3V_3H_4N_3Q_3]$-$[V_{94}I_6]$-{FIMYDP}-$[F_{83}W_{17}]$ {FIMYDP} represents any aa except FIMYDP		(Hendrickx *et al.*, 2009)
SILK motif		
Motif	**PIP**	**Reference**
K-[GS]-I-L-K	NOM-1 WBP11	(Huang *et al.*, 1999) (Gunawardena *et al.*, 2008)
[GS]-I-L-[RK] -X(7-107)-[RK]-X(0,1)-[VI]-{P}-[FW] X(7-107) means that SILK motif needs to be from 7 to 107 aa of distance from the RVxF motif; X(0,1) is any aa, present or absent**;** {P} represents any aa except P		(Huang *et al.*, 1999) (Llorian *et al.*, 2004)
Inhibitor-2 degenerate motif		
Motif	**PIP**	**Reference**
R-[KR]-X-H-Y X is any aa	I-2	(Yang *et al.*, 2000)
MyphoNE motif (N-terminal helicoidal element)		
Motif	**PIP**	**Reference**
R-X-X-Q-[VIL]-[KR]-X-[YW] X is any aa	MYPT1 MYPT2	(Terrak *et al.*, 2004)
Other motifs (help the binding but need also the RVxF motif)		
Motif	**PIP**	**Reference**
F-X-X-[RK]-X-[RK] X is any aa	Bcl-2 Bad Bcl-X Bcl-W	(Ayllón *et al.*, 2001) (Ayllon *et al.*, 2002)
R-A-R-A	GADD34	(Brush *et al.*, 2003)

PIPs are divided in four major categories: substrates, substrate-specific subunits, targeting subunits or inhibitors of the catalytic activity. (Bollen *et al.*, 2010). Some PIPs are PP1 substrates, for example, BRCA1 (Liu *et al.*, 2002), the focal adhesion kinase (FAK), the protein phosphatase CDC25C (Margolis *et al.*, 2003), the apoptotic protein Bad (Ayllon *et al.*, 2002), caspase 2 and protein kinases Nek2 (Li *et al.*, 2007). In opposition to the others, the last two are maintained in inactive state by PP1. Inhibitor-2 (Hurley *et al.*, 2007) and CPI-17 (Eto, 2009) are both substrates and inhibitors of PP1, and Nek2 (Wu *et al.*, 2007) and TIMAP (Csortos *et al.*, 2008) are dephosphorylated by PP1 but also target other proteins for PP1 mediated dephosphorylation. On the other hand, PIPs can target PP1 to specific structures such as the nucleus (TAT-1, PNUTS) (Allen *et al.*, 1998), nuclear membrane (AKAP149) (Steen *et al.*, 2003), nucleoli (NOM1) (Gunawardena *et al.*, 2008), chromatin (Repo-man) (Vagnarelli *et al.*, 2006), centrosome (Nek2) (Li *et al.*, 2007), plasma membrane (integrin αIIB), actin cytoskeleton (neurabin-I and neurabin-II) (MacMillan *et al.*, 1999), microtubules (TAU), myosin (MYPT1, MYPT2, MBS85, MYPT3 and TIMAP) (Terrak *et al.*, 2004), glycogen particles (GM, GL, R5/PTG, R6 and R3E), endoplasmic reticulum (GADD34, RIPP1) (Brush *et al.*, 2003), mitochondria (URI, Bcl2). Finally, some PIPs are true PP1 inhibitors, as they block the access to the active site and inhibit the dephosphorylation of all substrates, for instance inhibitor-2 and inhibitor-3 (Hurley *et al.*, 2007).

Additionally, several regulators show preferential binding to a specific PP1 isoform. Some examples are given in Table 2.

Table 2| PIPs whose function was described for a specific PP1 isoform.

Function	PIPs	Isoform Preference	Reference
Protein Synthesis	GADD34	PP1α	(Brush *et al.*, 2003)
	NIPP1	PP1α	(Eynde *et al.*, 1995) (Trinkle-Mulcahy *et al.*, 1999)
	Androgen-Receptor	PP1α	(Chen *et al.*, 2009)
Cell Cycle	Nucleolin	PP1β	(Morimoto *et al.*, 2002)
	PNUTS	PP1α	(Allen *et al.*, 1998)
	LCP1	PP1γ	(Trinkle-Mulcahy *et al.*, 2006)
	RIF1, isoform 4	PP1α	(Trinkle-Mulcahy *et al.*, 2006)
	NEK2A	PP1α	(Lou *et al.*, 2004)
	CAV1	PP1α	(Li *et al.*, 2003)
	Staufen	PP1α	(Brendel *et al.*, 2004)
Checkpoint Control and DNA Repair	BRCA1	PP1α	(Liu *et al.*, 2002)
	NPM	PP1β	(Lin *et al.*, 2010)
	Repo-Man	PP1γ	(Trinkle-Mulcahy *et al.*, 2006)
Cell Cycle Arrest and Apoptosis	p53BP2	PP1α	(Helps *et al.*, 1995)
	Bcl-2	PP1α	(Ayllón *et al.*, 2001)
	Bad, Bcl-X, Bcl-xL, Bcl-W,	PP1α	(Ayllon *et al.*, 2002)
	AKP1	PP1α	(Steen *et al.*, 2003)
	APAF1	PP1α	(Flores-Delgado *et al.*, 2007)
Cytoskeleton Dynamics	Neurabins	PP1γ1	(MacMillan *et al.*, 1999)
	KPI-2	PP1γ	(Cao *et al.*, 2002)
	MYPT family (except MYPT3)	PP1β	(Alessi *et al.*, 1992)
	MYPT3	PP1α	(Ito *et al.*, 2004)
	Phostensin	PP1α	(Trinkle-Mulcahy *et al.*, 2006) (Kao *et al.*, 2007)
	TAU	PP1γ	(Liao *et al.*, 1998)
Glycogen Metabolism	GM, GL, R5/PTG, R6, R3E	PP1β	(Johnson *et al.*, 1996)

Receptors Modulation	Glutamate receptors (mGlu1, mGlu5, mGlu7b)	PP1γ1	(Enz, 2002)
Testis Function	Endophilin B1t	PP1γ2	(Hrabchak *et al.*, 2007)
	TLRR	PP1γ2	(Wang *et al.*, 2010)
	HSPA5	PP1γ2	(Chun *et al.*, 1999)
	14-3-3-zeta	PP1γ2	(Puri *et al.*, 2008)
	NIPP1-T	PP1γ2	(Fardilha *et al.*, 2004)
Neuronal Function	AKAP9	PP1α	(Westphal *et al.*, 1999)
	DARPP32	PP1α	(Svenningsson *et al.*, 2004)
	N-Cor	PP1γ	(Hermanson *et al.*, 2002)
SR Ca(2+) cycling in cardiomyocytes	Phospholamban (PLN)	PP1β	(Aoyama *et al.*, 2011)
Other	Myopalladin	PP1α	(Trinkle-Mulcahy *et al.*, 2006)
	EWS	PP1α	(Trinkle-Mulcahy *et al.*, 2006)
	Taperin	PP1α	(Trinkle-Mulcahy *et al.*, 2006)

1.3.3. PP1 DISTRIBUTION AND EXPRESSION

It has already been shown that PP1 isoforms are expressed in a variety of mammalian cells, although they localize within these cells in a distinct and characteristic manner (Table 3). PP1 changes its phosphorylation status, activity, and subcellular localization during the cell cycle. Studying PP1 movement during the cell cycle, Andreassen *et al.* demonstrated that the distribution of PP1 isoforms in cells was highly dynamic. PP1 α, β and γ1 localize to distinct subcellular compartments during both interfase and mitosis (Andreassen *et al.*, 1998). PP1 is expressed in various cellular compartments, but it is most abundant in the nucleus. Within the nucleus, PP1α associates with the nuclear matrix, PP1γ1 localizes to the nucleolus, and PP1β is associated with whole chromatin. During mitosis, PP1α localizes to centrosomes, while PP1γ1 is associated with microtubules of the mitotic spindle. In contrast, PP1β is strongly localized to chromosomes (Trinkle-Mulcahy *et al.*, 2001; Trinkle-Mulcahy *et al.*, 2003; Anderson *et al.*, 2010).

PP1 isoforms vary in different brain regions and have also specific subcellular localization (da Cruz e Silva *et al.*, 1995; Strack *et al.*, 1999). While PP1β is the predominant isoform associated with microtubules in the neuronal cell body, PP1γ1 and PP1α are preferentially concentrated in the dendritic spines (Ouimet *et al.*, 1995; Strack *et al.*, 1999).

All four isoforms of PP1, α, β, γ1 and γ2, are expressed in mammalian testis (Table 3) (Chakrabarti *et al.*, 2007). However, its subcellular distribution in human testis is unknown.

Table 3| Tissue expression of PP1 isoforms.

PP1			
α	**β**	**γ1**	**γ2**
Ubiquitously expressed. More predominant in brain and lung. (Shima *et al.*, 1993)	Ubiquitously expressed. More predominant in brain, intestine and lung. (Shima *et al.*, 1993)	Ubiquitously expressed. More predominant in brain. Low levels in muscle and liver. (Shima *et al.*, 1993)	Predominantly in testis and sperm. Low abundance in other tissues. (Shima *et al.*, 1993; Barford *et al.*, 1998)
All isoforms are expressed in testis (Chakrabarti *et al.*, 2007; Fardilha *et al* 2011)			

1.3.4. PP1 AND TESTIS FUNCTION

The PP1γ gene undergoes tissue-specific splicing, giving rise to a ubiquitously expressed isoform, PP1γ1, and a testis-enriched and sperm specific isoform, PP1γ2. The strict difference between these two isoforms resides mainly in the carboxyl-terminus. Although isoforms typically display similar functional properties, especially when assayed *in vitro*, the fact that they are often differentially expressed, depending on the cell type or tissue, and also during development, suggests that they perform distinct, but sometimes overlapping, physiological functions (Kirchner *et al.*, 2007). This feature is evident in the PP1 isoform knockouts The PP1γ knockout mice are normal, although males are infertile due to impaired germ cell morphogenesis and apoptosis, leading to the absence of epididymal spermatozoa (Figure 7) (Varmuza *et al.*, 1999). So, all PP1γ functions were compensated by the other PP1 isoforms except for male fertility (Chakrabarti *et al.*, 2007). These findings demonstrate the isoform-specific role of PP1γ2, the predominant PP1 isoform in male germ cells, in mammalian spermatogenesis. Although the PP1γ2 specific targets remain unknown and the complexity of Ppp1cc null mice phenotype suggests that this protein may affect a number of pathways within the testis.

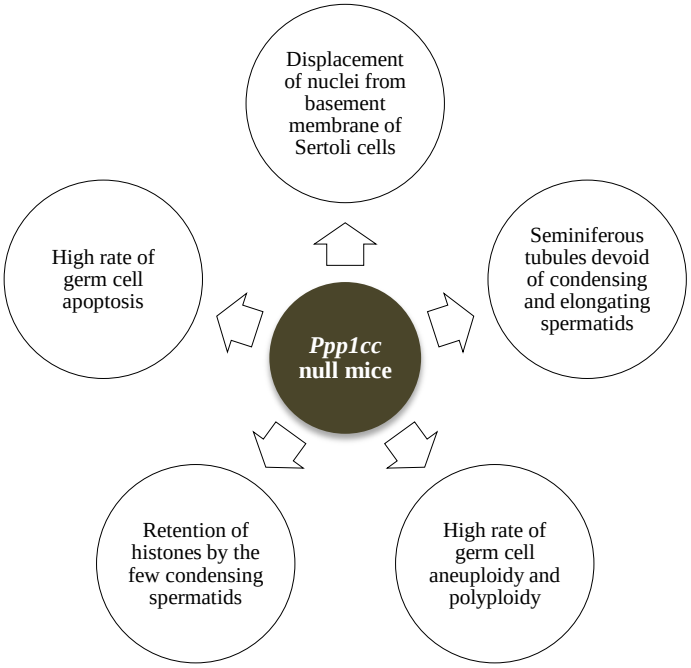

Figure 7| The *Ppp1cc* null phenotype affects both the germ cells and the somatic Sertoli cells within the seminiferous tubules (Jurisicova *et al.*, 1999; Varmuza *et al.*, 1999; Oppedisano *et al.*, 2002). The phenotype of the mutant mice resembles the human patients suffering from testicular failure, and consequently can serve as a useful model for study infertility in humans.

1.3.4.1. TESTIS/SPERM-SPECIFIC PIPS

Some testis/sperm-specific PIPs have been identified, for instance, the spermatogenic zip protein 1 (Spz1) (Hrabchak *et al.*, 2004). Overexpression of Spz1 and loss of PP1γ in the testis show similar phenotypes (spermatogenic arrest and germ cell apoptosis) (Hrabchak *et al.*, 2004) (Table 4). Other proteins that have also been implicated in the regulation of PP1γ2 in testis/sperm are 14-3-3 zeta (induce PP1γ2 activity during sperm maturation) or sds22 and hsp90 (inhibited PP1γ2 activity during sperm maturation) (Table 4) (Huang *et al.*, 2002; Hrabchak *et al.*, 2004; Huang *et al.*, 2004; Huang *et al.*, 2005). The testis enriched isoform endophilin B1t was demonstrated to bind PP1γ2, but did not bind PP1γ2 mutated in the C-terminus, nor PP1α (Table 2). Moreover, the characteristic expression pattern of endophilin in testis was absent in PP1γ null mice (Hrabchak *et al.*, 2007). In another study, Cheng *et al* showed a direct reciprocal relationship between the levels of the protein phosphatase isoform PP1γ2 and its regulator inhibitor-3 (I3), and suggest that complex formation between these polypeptides in testis may prevent proteolysis of I3 and thus, germ cell apoptosis (Cheng *et al.*, 2009). The A-kinase anchoring proteins (AKAPs), as PIPs, have been also related to testis and sperm function, specifically AKAP3, AKAP4 and AKAP220 (Table 4) (for review see Fardilha, 2011 #555).

Table 4 | Some known testis/sperm-specific PIPs.

PIPs	Subcellular Localization in Sperm	Function	References
SpzI	-	Spermatogenesis	(Hrabchak *et al.*, 2004)
14-3-3 zeta	Post-acrosome, Principal piece	Spermatogenesis Sperm maturation	(Huang *et al.*, 2004)
Hsp90		Sperm maturation	(Huang *et al.*, 2005)
Sds22	Connecting piece Principal piece	Sperm maturation	(Huang *et al.*, 2002)
Endophilin BIt	-	-	(Hrabchak *et al.*, 2007)
I2	Tail	Motility	(Vijayaraghavan *et al.*, 1996)
I3	Head Principal piece	Spermatogenesis	(Lesage *et al.*, 2007)
AKAP3/AKAP110/ FSP95/SOBI	Principal piece, fibrous sheath, acrosome	Acrosome reaction, sperm motility	(Vijayaraghavan *et al.*, 1997) (Vijayaraghavan *et al.*, 1999)
AKAP4/AKAP82/ FSCI	Principal piece, fibrous sheath	Sperm motility	(Visconti *et al.*, 1997)
AKAP11/AKAP220	Cytoplasm, centrosome, middle piece	Sperm maturation, motility	(Vijayaraghavan *et al.*, 1997)

1.3.4.2. ALTERNATIVE SPLICING IN TESTIS

Alternative splicing appears to be a common strategy for generating diversity in the testis. Like PP1γ2, many testis-expressed genes undergo alternative splicing. For instance, Nek2 variants, Nek2A and Nek2C (Wu *et al.*, 2007), as well as a new splice variant of NIPP1 designated NIPP1-T (Fardilha *et al.*, 2004) and SARP2 (Browne *et al.*, 2007), which were identified in Yeast Two-Hybrid (YTH) screens of human testis cDNA libraries using PP1γ1 and PP1γ2 as baits (Fardilha *et al.*, 2004), were shown to be highly expressed in human testis. These testis-specific alternatively spliced proteins are interesting targets for the development of new therapeutic strategies for male infertility and contraception.

1.3.5. SARP – A PP1 INTERACTING PROTEIN

PIPs are responsible for controlling PP1 activity, therefore understanding the function of PP1 lies in identifying the cellular roles of these PIPs. In order to identify and define the properties of PIPs in human testis, YTH screens of a human testis cDNA libraries, using PP1γ1, PP1γ2 as baits were performed (Fardilha *et al.*, 2011). Several new interactions, apart from previously known PIPs, were identified. One of the PIP identified was a new protein termed SARP (several ankyrin repeat protein) (Browne *et al.*, 2007). Bacterially expressed SARP was found to bind bacterially expressed PP1γ1 and PP1γ2 by immunoadsorption and blot overlay experiments respectively, and endogenous PP1γ2 was found to complex with SARP2 in human sperm (unpublished data). SARP interacts not only with all isoforms of PP1, but also with DNA. A region encompassing a consensus PP1-binding motif in SARP (354KVHF357), which lies partially within the first ankyrin-repeat domain, modulates SARP–PP1 activity in mammalian cells.

Three isoforms, resulting from a single gene located on chromosome 11 by alternative splicing, have been identified. SARP1 and SARP2 (92–95 kDa) (Figure 8) are ubiquitously expressed in all tissues with high levels in testis and sperm, where they interact with PP1γ2. SARP1 and SARP2 contain eight ankyrin repeats, a putative leucine-zipper domain and a putative Ca^{2+} binding EF-hand. On the other hand, SARP3 (65 kDa), contains six ankyrin repeats and is more abundant in brain where it interacts with both PP1α and PP1γ1 (Browne *et al.*, 2007).

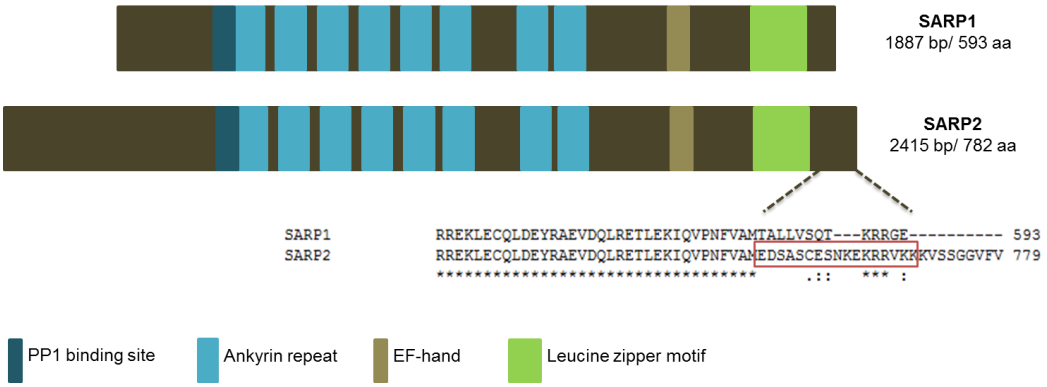

Figure 8| Schematic representation of the SARP1 and SARP2 amino acid sequences derived from cDNAs, DQ508815 and EF041819, respectively. The homology analysis of SARP isoforms C-terminal was performed using a CLUSTALW2 multiple sequence alignment. The red box in the C-terminal indicates the peptide used to generate SARP2 antisera in rabbit.

Most regulatory subunits of PP1 share little or no obvious sequence similarities unless they are isoforms, the canonical PP1-binding motif and the ankyrin-repeat domain found in SARP is observed in three other known PP1-associated proteins: p53BP2, TIMAP and MYPT.

The presence of a putative nuclear localization signal (NLS) at the N-terminus suggests that SARP functions within the nucleus. PP1 interacts with several proteins that modulate transcription. For example, homeodomain transcription factor Hox11, host cell factor HCF, the retinoblastoma protein p110Rb and p53BP2. Moreover SARP1 and 2 have a putative leucine-zipper motif near the C-terminus, a domain found in many transcription factors, and SARP2 specifically binds to mammalian DNA. Both facts suggest that SARP1 and SARP2 may function as transcription factors or DNA-associated proteins that modulate gene expression (Browne *et al.*, 2007).

Furthermore, SARP2 possesses an EF-hand type Ca^{2+} binding motif and it is well established that Ca^{2+} is pivotal in controlling motility and chemotaxis in mammalian sperm (Publicover *et al.*, 2007). Sperm possesses an unique calcium-permeable CatSpers (sperm cation channels), restricted to flagellum and regulated primarily by pH. Plasma membrane calcium ATPase4 (PMCA4) is also restricted to the flagellum. If SARP proves to bind Ca^{2+}, it may constitute an excellent candidate for a protein involved in bridging phosphorylation and calcium signaling in sperm cells.

1.4. AIMS

The aim of this study was to identify the cellular and subcellular localization of PP1 isoforms and SARP2 in human testis in order to clarify the role of these proteins in testis. To that end we proposed to:

1. Obtain human testis and epididymis biopsies;
2. Process the human samples for immunohistochemistry, electron microscopy and immunoelectron microscopy;
3. Analyze the ultrastructure of human testis and epididymis by electron microscopy;
4. Analyze the human samples for the localization of PP1 isoforms at different steps of spermatogenesis by immunoelectron microscopy and fluorescence microscopy;
5. Analyze the human samples for the localization of SARP2 at different steps of spermatogenesis by immunoelectron microscopy and fluorescence microscopy.

2. ULTRASTRUCTURE ANALYSES OF THE HUMAN TESTIS AND EPIDIDYMIS

2.1. MATERIAL AND METHODS

Experimental procedures were performed in Signal Transduction Laboratory, Center for Cell Biology, University of Aveiro (Aveiro, Portugal) and in Justus-Liebig-Universität, Institut für Anatomie und Zellbiologie (Giessen, Germany). The details of the solutions used in this thesis are stated in the appendix.

2.1.1. HUMAN SAMPLES COLLECTION

Human testis and epididymis biopsies were collected *in vivo*, in Hospital Central (Centro Hospitalar de Coimbra), during procedures to collect organs for transplantation from adult man donors, and in Ferticentro, in the course of a testis biopsy for a fertility study. During the biopsies, the different regions of both testis and epididymis were collected *in vivo*. In Ferticentro, the samples were collected from the middle third of the anterior portion of the right testis, after written informed consent was given.

2.1.2. ELECTRON MICROSCOPY

2.1.2.1. FIXATION AND POST-FIXATION

For electron microscopy analyses, after the collection, the human biopsies (testis and epididymis) were immediately immersed in fixative A and B (see appendix). The samples were maintained in the fixative overnight (ON), in order to achieve complete fixation (Figure 9). Then, the tissue was transferred into the appropriate buffer (A or B, see appendix). After fixation, the samples were post-fixed in 1% aqueous osmium tetroxide ON (Figure 9). Osmium tetroxide is used as a secondary fixative after aldehyde fixation because its rate of penetration is too slow to prevent artifacts if used initially. Osmium tetroxide reacts primarily with lipid moieties, oxidizing unsaturated bonds of fatty acids. This reduced heavy metal adds density and contrast to the biological tissue. It also acts as a mordant enhancing lead staining. Osmium tetroxide is toxic and volatile fumes are very corrosive, especially to mucous membranes, therefore, it should be handled carefully.

2.1.2.2. DEHYDRATION AND EMBEDDING

The samples were dehydrated in a series of graded ethanol (70%, 80%, 90%, 100%, 3 times, 15 min each step). Samples were then incubated with propylene oxide (transitional solvent) (3 times, 5 min each) and then in a 1:1 mixture of propylene oxide and epon resin (Agar 100 Resin kit, Agar Scientific Ltd., Essex, United Kingdom) for 30 min. Propylene oxide was used to remove residual ethanol previously used for dehydration. The specimen was then transferred to fresh epon resin at 4°C, ON. Finally, the tissue was embedded in medium grade epon resin and allowed to polymerize at 60°C for 48 hours (Figure 9).

To make the epon resin, the required amounts of warm resin (Agar 100) and hardeners (DDSA and MNA) were measured into a warm graduated cylinder and poured into the warm conical flask. The mixture was mixed gently and then the accelerator (BDMA) was added.

2.1.2.3. SECTIONING, CONTRAST STAINING AND OBSERVATION

Semi-thin sections (1µm) were prepared and stained with Rudeberg solution for the selection of the regions of interest in the light microscope, then 80 nm ultrathin sections were cut on LEICA microtome (VT1000S), collected on 100 mesh nickel grids, and thereafter coated on the back side with a 1% formvar film (support film). After contrasting with uranyl acetate for 2 min and lead citrate (Reynolds solution) for 45 sec, the samples were inspected in a LEO 906 electron microscope (see appendix, Figure 30) (Figure 9).

Figure 9| Electron microscopy procedure overview. Theoretically, a 0,5% glutaraldehyde fixation solution is more appropriated to preserve tissue ultrastructure. The post-fixation procedure (blue boxes) is only used in electron microscopy. Osmium tetroxide forms cross-linked complexes with many organic compounds, and in the process becomes reduced. This reaction is useful for fixing cell membranes, since the carbon double bonds, present in many fatty acids, react with osmium tetroxide. (ON, overnight; min, minutes; sec, seconds)

2.2. RESULTS

2.2.1. TESTIS SEMI-THIN SECTIONS AND ULTRA-THIN SECTIONS

Semi-thin sections (1µm) stained with Rudeberg solution were analysed by light microscopy, for the selection of regions of interest for further (immuno)electron microscopy studies. Figure 10 shows a light micrograph of human testis seminiferous tubules. The seminiferous tubules are highly convoluted and lined by a stratified epithelium which consists of cells in various stages of spermatogenesis (collectively referred to as the spermatogenic series).

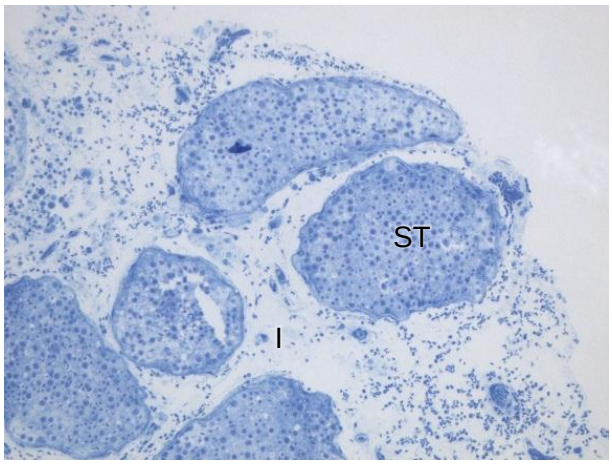

Figure 10| Light micrograph of human testis seminiferous tubules (ST; cut in various planes of section), and the interstitial tissue (I).

After selecting the regions of interest, the human testis ultrathin-sections (80 nm) were collected on 100 mesh nickel grids (Figure 11).

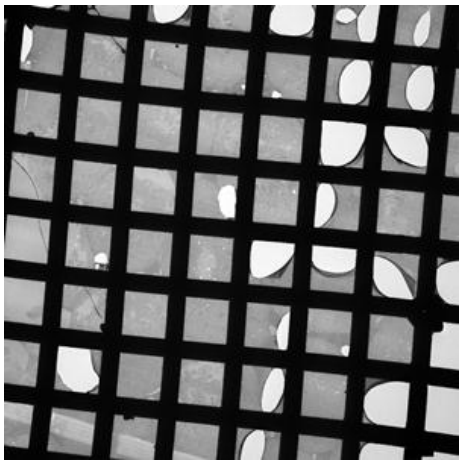

Figure 11| Electron micrograph view of testis ultrathin sections collected on a 100 mesh nickel grid, and coated with a support film (1% formvar film).

2.2.2. ELECTRON MICROSCOPY ANALYSES OF HUMAN TESTIS

Detailed ultrastructural analysis of ultrathin sections of human testis by TEM was performed. Results in this section (2.2.2) show optimal tissue preservation with both fixatives tested.

2.2.2.1. TESTIS OVERVIEW

The overview from the seminiferous tubules (Figure 12) shows spermatogonia, spermatocytes and spermatids with normal nuclear and cytoplasmic features. It is also possible to observe mature spermatozoa in the tubule's lumen.

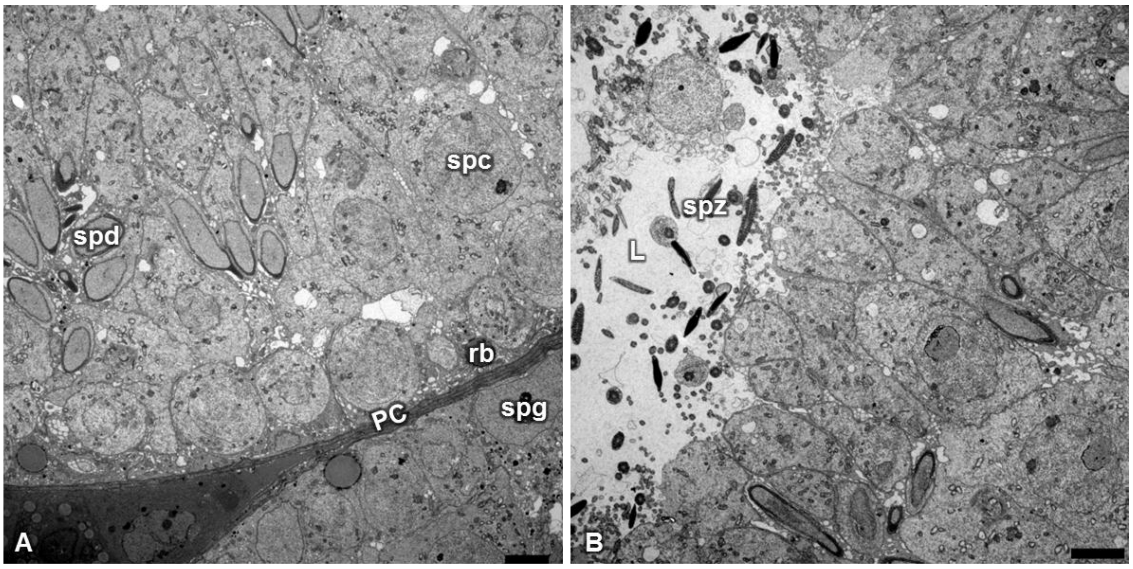

Figure 12| Electron micrographs of an overview from the seminiferous tubules containing germ cells of various stages, covering the entire process of spermatogenesis. Peritubular myoid cells (PC); Spermatogonia (spg); Spermatocyte (spc); Spermatid (spd); Spermatozoa (spz); Residual body (rb); Cytoplasmic droplet (cp); Lumen (L). Bars represent 5000 nm. A and B: Fixative A.

2.2.2.2. BASAL COMPARTMENT

In Figure 13 the basal compartment of a seminiferous tubule is analysed by electron microscopy. Figure 13 shows the two types of spermatogonia, type A spermatogonia with an ovoid nucleus that stains darky (A dark) or pale (A pale) and type B spermatogonia characterized by spherical nuclei, consistent with greater differentiation and commitment to meiosis.

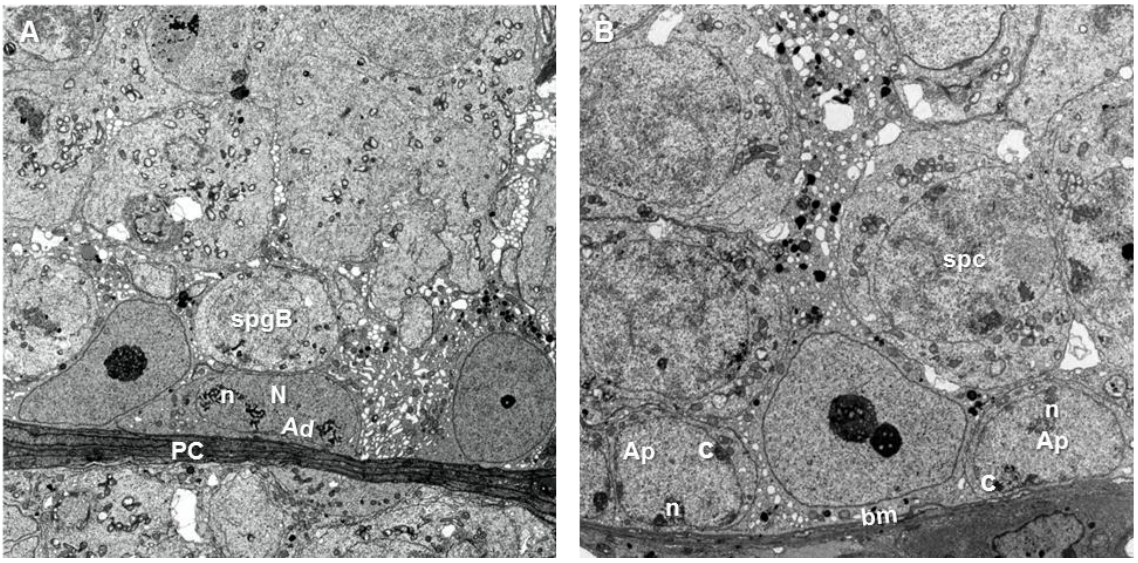

Figure 13| Electron micrographs of a seminiferous tubule basal compartment. The seminiferous tubules are surrounded by thin plate-like contractile cells - peritubular myoid cells (PC). Type A dark spermatogonia (Ad) shows a dark oblong nucleus (N) and a prominent nucleolus (n) while the more differentiated type A pale spermatogonia (Ap) accumulate progressively more chromatin (c) on the nuclear membrane, gradually take an ovoid nuclear shape (type B spermatogonia, spgB), and show prominent nucleoli as they advance in maturation. More undifferentiated spermatogonia contacts the basement membrane (bm). Spermatocyte (spc) reveling a spherical nucleus (N). A and B: Fixative A.

2.2.2.3. SERTOLI CELL

The characteristics of Sertoli cells are depicted in Figure 14 which enables us to conclude that these cells are columnar in height and extend thin cytoplasmic processes between the developing germ cells.

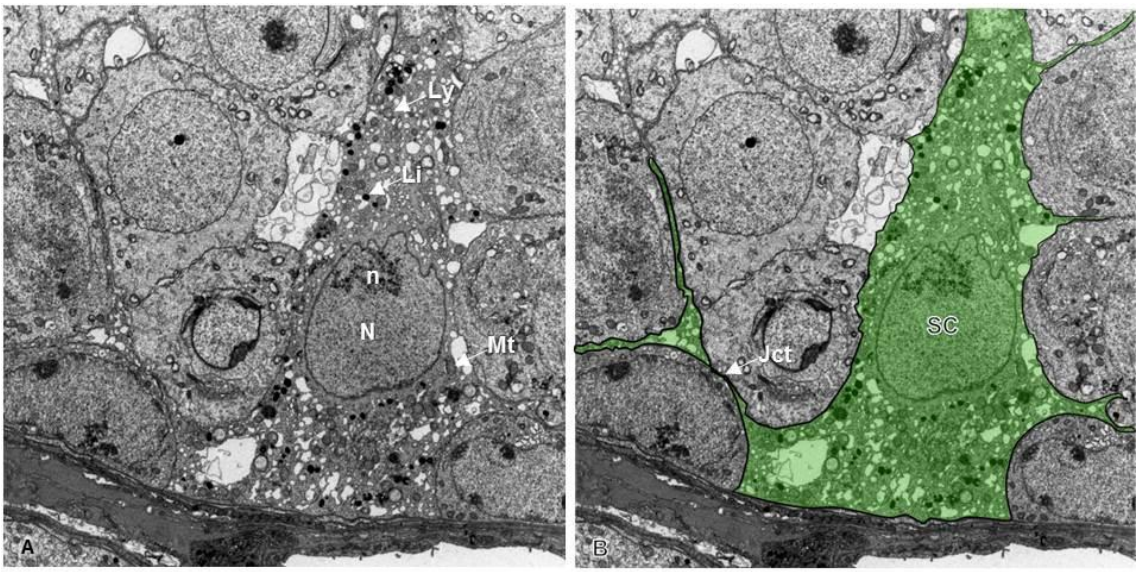

Figure 14| Electron micrographs of the Sertoli cell. Sertoli cell is columnar in height and extend from the basement membrane (bm) to the lumen and have specialized junctional complexes (Jct). The nucleus (N) is found near the base of the cell and contains a large nucleolus (n). Lipid droplets (Li) can be noted. Note the thin cytoplasmic processes that extend between the developing germ cells (Sertoli cell is enhanced with green color in B). The cytoplasm contains several organelles and inclusion bodies, such as mitochondria (Mt) and lysosomes (Ly). A and B: Fixative A.

2.2.2.4. LEYDIG CELL

Human Leydig cells, within the intertubular and adjacent to blood vessels, are showed in Figure 15.

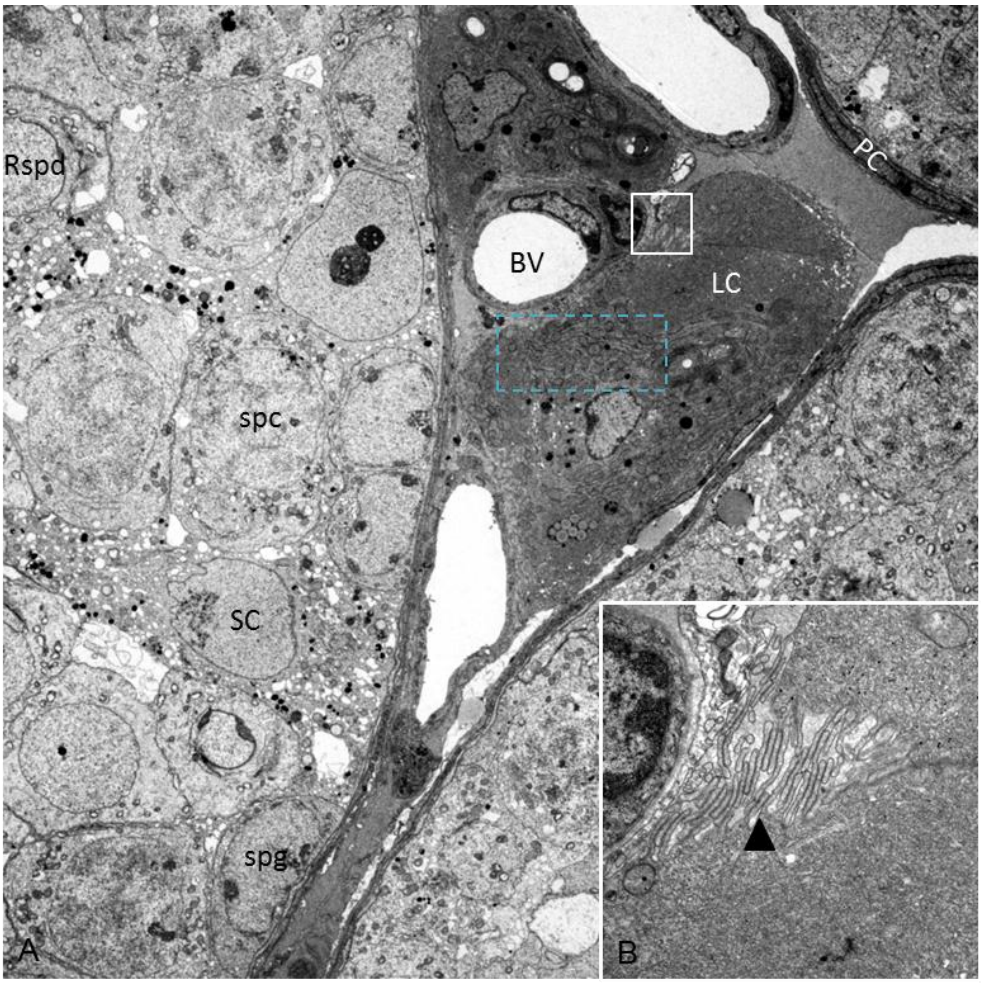

Figure 15| Electron micrographs of the Leydig cell. Leydig cells contains abundant smooth endoplasmic reticulum (sER) (B shows a higher magnification (arrow)) and mitochondria (dashed blue box) which have tubular cristae typical to steroidogenic cells. spg, spermatogonia; spc, spermatocyte; Rspd, round spermatid; SC, Sertoli cell; PC, peritubular cell; BV, blood vessels. A and B: Fixative B.

2.2.2.5. SPERMIOGENESIS

In Figure 16 is possible to observe the structural and functional changes occurring within developing spermatids, such as major modifications in the shape of the cell and nucleus, compaction and condensation of the nuclear chromatin, development of the acrosome on the nucleus surface, and elimination of the excess cytoplasm of the spermatids.

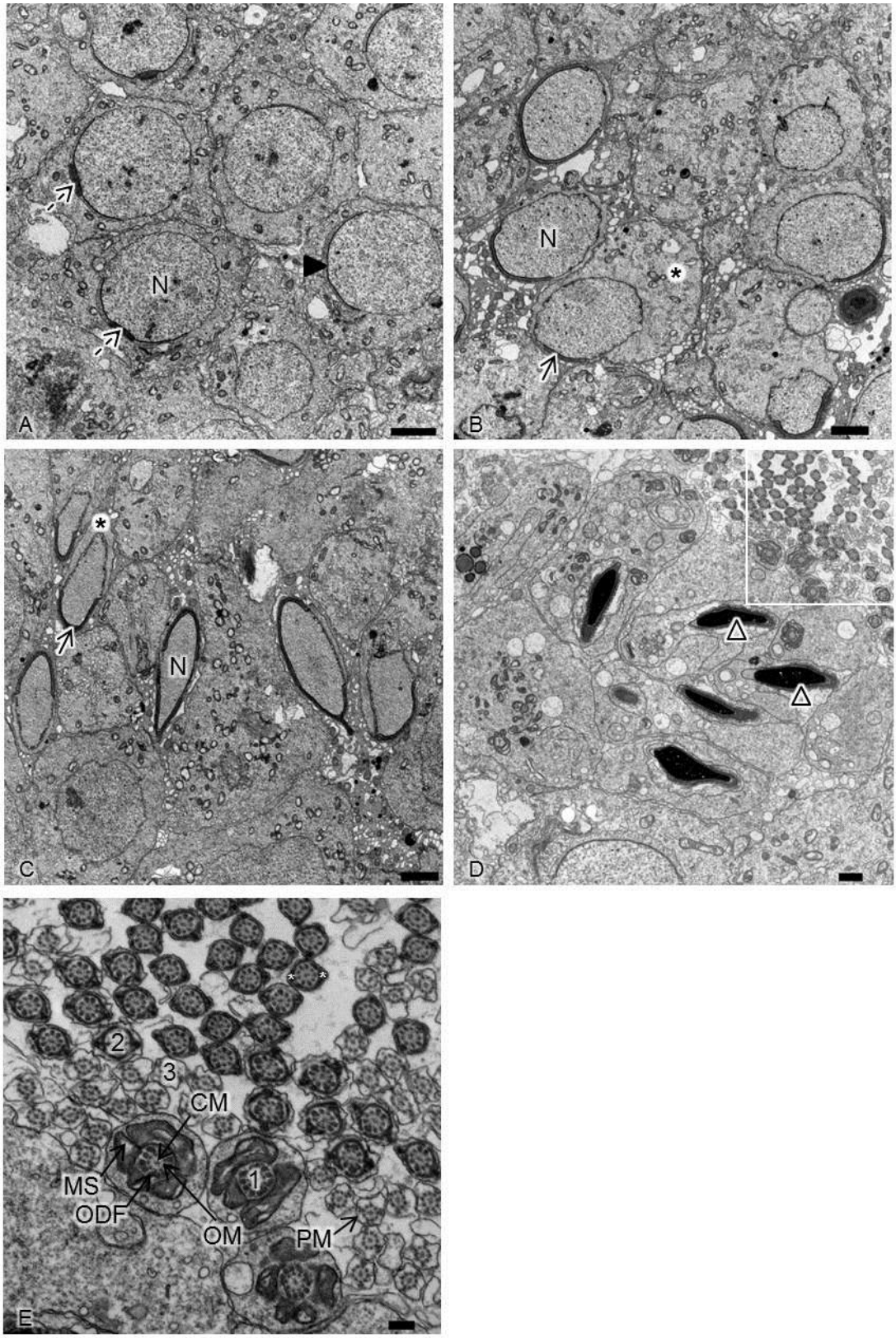

Figure 16| Electron micrographs of the changes involving the transformation of round spermatids into spermatozoa. Modification of the nucleus (N) from spherical in round spermatids (A) to sickle-shaped (C); nuclear chromatin becomes compacted (D); beginning of the acrosome formation (A, dashed arrow) on one pole of the nucleus that becomes applied as a cap-like structure over approximately 30-50% of the nuclear

surface (A, arrowhead); change in shape of the cytoplasm from spheroidal (A) to an elongated form called the cytoplasmic lobe (B and C, *); nucleus comes into close opposition with the cell membrane in the region that is covered by the acrosomal cap (B and C, arrow). In D it is possible to see cross sections of sperm heads, which shows a nucleus highly condensed (arrowhead), and through the sperm tail mid-piece, principal piece and end piece. E shows a higher magnification of the ultrastructural subdivisions of the flagellum from D. The mid-piece (1) presents 9 outer dense fibers (ODFs) surrounding each of the 9 outer axonemal microtubules doublets (OM) which in turn surround a pair of microtubules in the central region (CM), and a mitochondrial sheat (MS), which is restricted to the mid-piece, that encloses the ODFs and the axoneme. The principal piece (2) shows that the MS terminates and 2 of the ODFs are replaced by 2 longitudinal columns of fibrous sheath (FS; *). The FS are stabilized by circumferential ribs that surround the ODFs. The FS is restricted to the principal piece. The end piece (3) is the short terminal portion of the flagellum and has only the axoneme surrounded by the plasma membrane (PM). Bars represent: 2500 nm. A-E: Fixative A.

2.2.3. ELECTRON MICROSCOPY ANALYSES OF THE HUMAN EPIDIDYMIS

In the present work we also characterized using, electron microscopy, the ultrastructure of the human proximal epididymis epithelium, collected *in vivo* (Figure 17). These results show optimal epididymis tissue preservation with both fixatives tested.

The efferent duct system is lined by an epithelium of ciliated and principal columnar cells (Figure 17; A, F and G). The principal cells have round or oval euchromatic nucleus which occupies the basal half of the cell. The ciliated cells have elongated oval heterochromatic nuclei that are found mostly in the luminal half of the cell. Both cell types possess numerous organelles: Golgi complex, mitochondria and rough endoplasmatic reticulum. Apical mitochondria-rich ciliated cells with a more apically-located nucleus than principal cells are observed. Additionally, principal cells contain a plethora of vesicles varying in density and vacuoles - morphological features of cells involved in absorption and secretion (Figure 17; A, F and G). Figure 17 also shows evidences of secretory activity in non-ciliated cells (D, E and H).

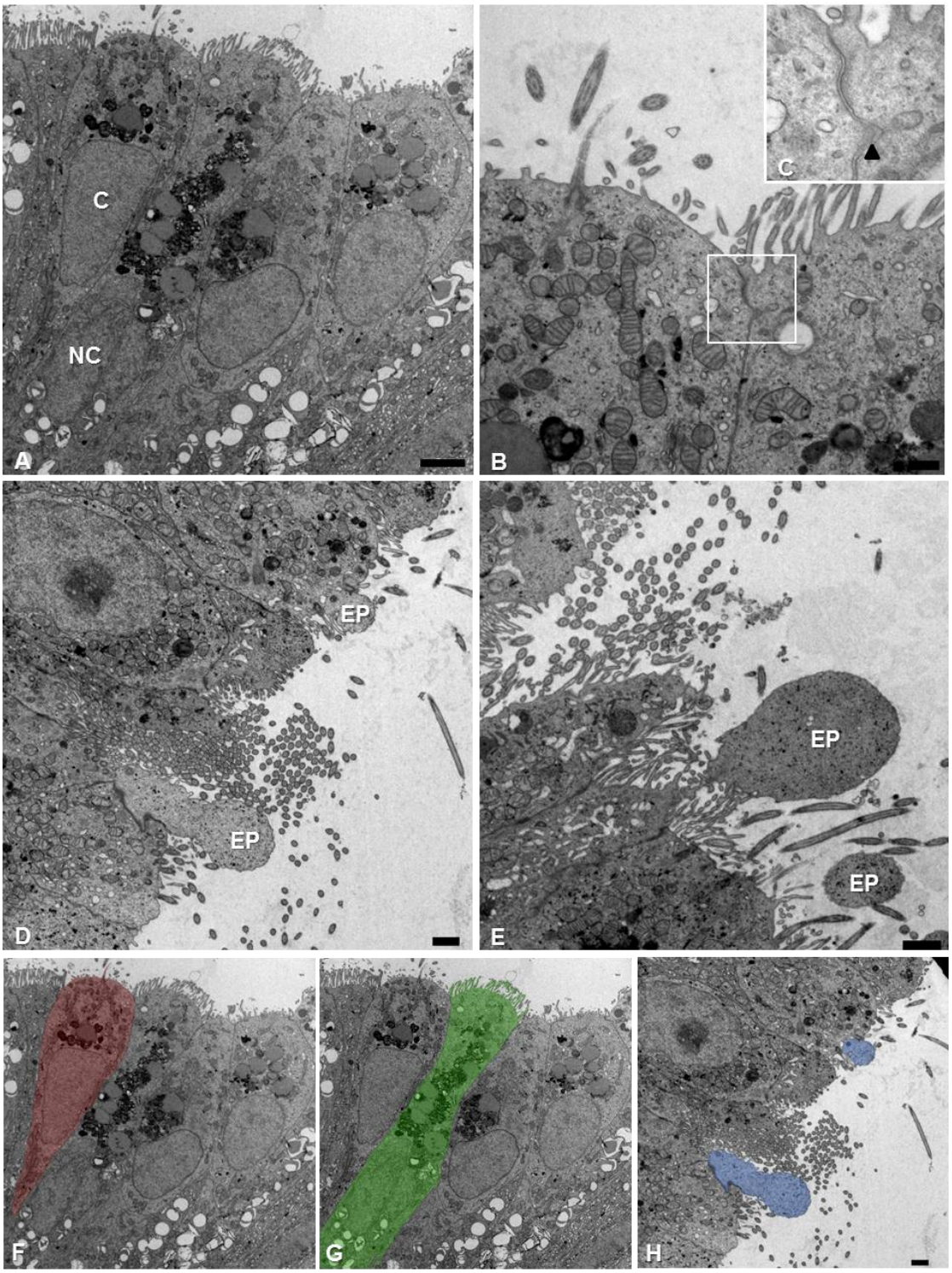

Figure 17| Electron micrographs of the human epididymis. In A we observe the cilia and the microvilli projected from the luminal surface of the ciliated (C) and principal (NC) cells into the ductular lumen, respectively. In B and C (higher magnification of B) it is possible to observe the tight junctions between the lateral plasma membrane of the two adjacent cells (blood-epididymis-barrier). D and E shows evidences of the apocrine secretion in the principal cells. The apical protrusions are designated epididymosomes (EP). F – Ciliated cell enhanced with red color. G – Principal cell enhanced with green color. H – Epididymosomes formation enhanced with blue color. Bars represent in A, F and G: 2500 nm; B: 500 nm; C: 250 nm; D, E and H: 1000 nm. A-H: Fixative A.

2.3. DISCUSSION

Understanding the ultrastructure of tissues is important to assess the tissue preservation status and correctly interpret immunoelectron microscopy images. For electron microscopy studies we tested two fixation methods: fixative A [higher concentration of glutaraldehyde (0,5%); paraformaldehyde (1%); pircric acid (0,025%); cacodylate buffer] and fixative B [lower concentration of glutaraldehyde (0,05%); paraformaldehyde (4%); sucrose (2%); HEPES buffer] followed by post-fixation with osmium tetroxide. Supposedly, fixative A is more appropriated to preserve tissue ultrastructure, due to its high glutaraldehyde content, and therefore, more suitable for electron microscopy studies. On the other hand, fixative B is more indicated to preserve antigenicity, hence, more suitable for immunoelectron localizations. Our results indicate that an optimal preservation of human testis and epididymis ultrastructure can be achieved with both fixatives.

Glutaraldehyde, picric acid and osmium tetroxide can have a deleterious effect on immunolabelling efficiency. Glutaraldehyde, a di-aldehyde containing two free aldehyde groups, can bind to cellular components with both of these aldehyde groups. It is by binding to cellular components, such as amino acid side-chains that extreme cross-linking occurs bringing good preservation of the ultrastructure, but possible loss of immunolabelling efficiency. Nevertheless, not all antigens are affected by glutaraldehyde (see section 4.4.) (Oliver, 1994). Picric acid, which stabilizes tissue structure to a higher degree, was used in one of the fixation solution. For optimal ultrastructure preservation, this primary fixation step was followed by fixation in osmium tetroxide. Osmium tetroxide fixes cellular lipids, especially those forming part of the cell membrane. All of these lipid-rich structures are poorly preserved by glutaraldehyde and paraformaldehyde. However, the use of osmium tetroxide was not used to immunolocalizations since it is not advised.

Dehydration is necessary since the embedding solutions are not miscible in water. The choice of the embedding agent is mainly important for optimal immunolabelling. In the present study, the embedding medium of choice was an Epoxy resin for ultrastructure studies and LR White for immunolocalizations.

2.3.1. HUMAN TESTIS

Ultrastructural analysis of the testis showed that the germ cells (Figure 18), Sertoli cells and Leydig cells had cellular characteristics typical of active spermatogenesis. It was also possible to confirm that the tissue is well preserved.

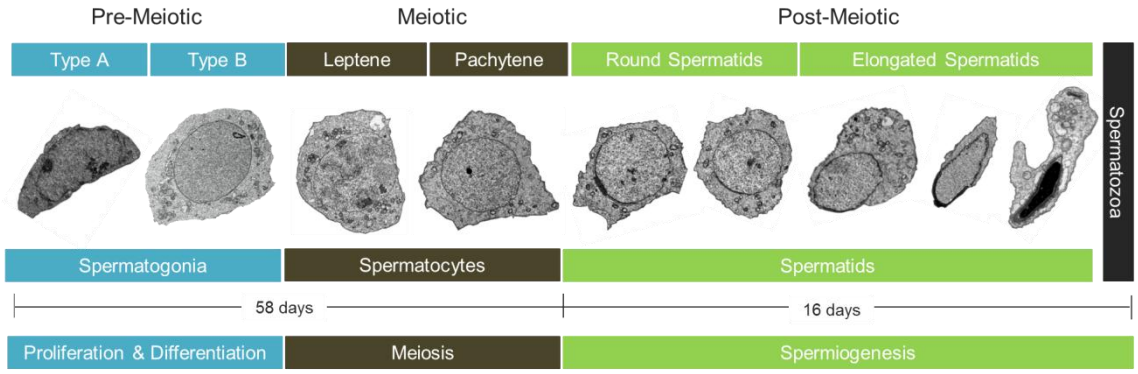

Figure 18| The electron microscopy study allowed us to characterize and understand the ultrastructure of the germ cells at different stages of maturation.

The Sertoli cells showed characteristics consistent with a secretory cell. The nuclei were irregular, with deep indentations and defined nucleoli. Adjacent to the nuclei, the cytoplasm was characterized by lipid droplets, mitochondria and glycogen granules dispersed throughout the cytoplasm. The plasma membranes were conspicuous and tortuous, showing close associations with adjacent germ cells (Figure 14).

Leydig cells showed distinct cytoplasmic characteristics, such as prominent lipid bodies, defined vesicles of smooth endoplasmic reticulum and mitochondria surrounding the nucleus (Figure 15).

2.3.2. HUMAN EPIDIDYMIS

The ultrastructure analyses revealed that the human epididymis is lined by an epithelium of ciliated and principal columnar cells (Figure 17, A, F and G)). These findings were similar to those described for rat (Hoffer, 1972), mouse (Hoffer, 1972), guinea pig (Hoffer *et al.*, 1978), and hamster (Flickinger *et al.*, 1978), among others. Additionally the ultrastructure analyses of the human epididymis, collected *in vivo*, revealed evidences of secretory activity in principal cells. An unconventional protein secretion, referred as apocrine secretion, has been proposed in the epididymis (Aumüller *et al.*, 1999). Unlike merocrine secretion, where secretory vesicles fuse with the apical membrane and the products are released outside the cell, the apocrine secretion is characterized by loss of the apical cytoplasm of the cells with the product of secretion. Apocrine secreted proteins share several peculiarities: (1) their biosynthesis and post-translational modification (including an unusual form of glycosylation) occurs in the cytoplasm (Aumüller *et al.*, 1999), (2) intracellular transport proceeds without participation of either the endoplasmic reticulum–Golgi apparatus complex or the secretory vesicles that fuse with the plasma membrane to liberate their content in the extracellular compartment as it occurs during merocrine secretion (Sullivan *et al.*, 2007), (3) blood serum derived albumin entering the secretory cells functions as a carrier of the apocrine-released proteins, (4) their primary sequence is synthesized without a signal peptide, (5) their N-terminus is blocked by acetylation (Aumüller *et al.*, 1999), (6) some contain a glycerol-phosphoinositol (GPI-) anchor (Sullivan *et al.*, 2007) and (7) their release in the lumen implicates the formation of "apical bleed". Those "apical bleeds" are shown in Figure 17 (D, E and H). The characterization and functions of the apical protrusions, or epididymosomes, remain largely unknown and these findings open new fields for understanding the human epididymis physiology (Figure 19). As shown previously, the epididymal epithelium has high protein synthesis and secretion activity and most of the proteins present in the epididymal fluid are hydrophobic proteins. These proteins are almost never present in the soluble form in epididymal fluid but partly associated with membrane structures such as epididymosomes (Frenette *et al.*, 2002; Gatti *et al.*, 2005). There are a number of still open questions regarding apocrine secretion, such as (1) the intracellular transport and targeting of the proteins, (2) the coordination of simultaneously occurring apocrine and merocrine secretion and (3) the repair mechanisms of the apical cell membrane following the release of the epididymosomes.

Modern and non-invasive contraceptive methods for men are still not available. An ideal male contraceptive should allow normal hormone production and spermatogenesis but should prevent the post-testicular sperm maturation, thus the epididymis appears to be a potential target. The role of the epididymal luminal microenvironment and the mechanisms that the epididymis uses to carry

out its functions remains unsolved. The majority of novel insights on epididymal biology and function resulted from animal models and vasectomized men or with testicular cancer. Moreover, there is variation between species in the structure of the different epididymal segments, suggesting some difference in the post testicular maturation. Additionally, the pattern of sperm surface proteins modification is species-specific (Dacheux *et al.*, 2009). All these facts emphasize the need of further studies using human tissue.

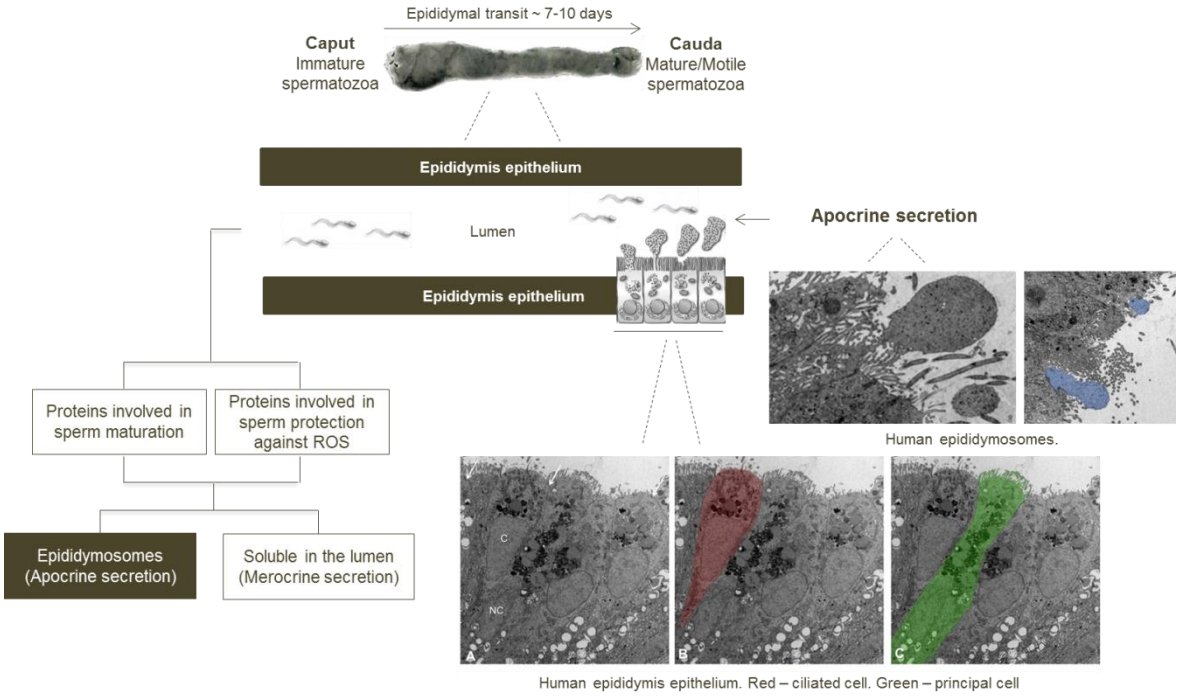

Figure 19| Within the epididymal lumen, spermatozoa interact with small membranous vesicles - epididymosomes. Many proteins are associated with epididymosomes and the protein composition of these vesicles varies along the duct and differs from soluble intraluminal proteins (Koppers *et al.*, 2011). Here, we show the ultrastructure of the epididymosomes, secreted in an apocrine manner by the human epididymal epithelial cells.

3. LOCALIZATION OF PP1 ISOFORMS AND SARP2 ON HUMAN TESTIS

3.1. MATERIAL AND METHODS

Experimental procedures were performed in Signal Transduction Laboratory, Center for Cell Biology, University of Aveiro (Aveiro, Portugal) and in Justus-Liebig-Universität, Institut für Anatomie und Zellbiologie (Giessen, Germany). The details of the solutions used in this thesis are stated in the appendix.

3.1.1. ANTIBODIES

Study of PP1 and SARP isoforms relies on the availability of highly specific antibodies (Figure 8; Figure 20). The amino acid sequences of the four PP1 isoforms (α, β, γ1 and γ2) are highly similar (> 90% identity overall), except for the N and C-terminal amino acids. Therefore, C-terminal sequences were chosen to generate antipeptide antibodies that would discriminate between the different PP1 isoforms (Figure 20) (da Cruz e Silva *et al.*, 1995). The specificity of the antibodies to PP1 isoforms was previously demonstrated as well as their utilization for immunohistochemistry and electron microscopy (da Cruz e Silva *et al.*, 1995; Ouimet *et al.*, 1995).

In Figure 8, the red box indicates the SARP2 unique C-terminal used to generate SARP2 antisera in rabbit. The SARP2 antibody specificity in human testis will be analyzed.

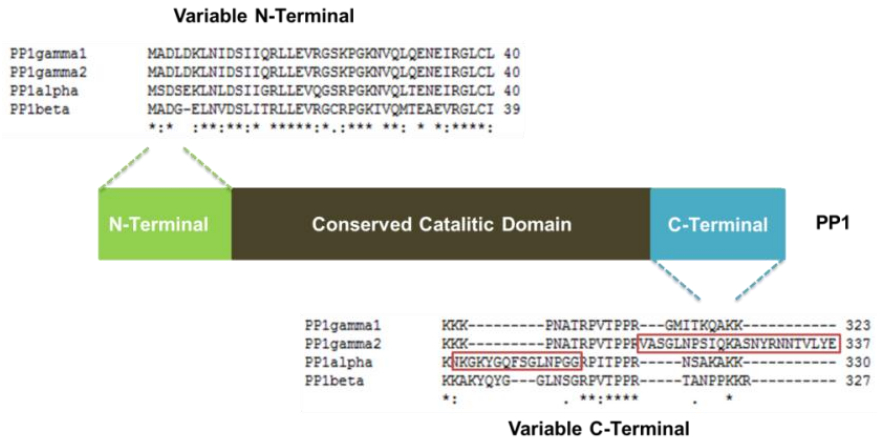

Figure 20| Schematic representation of divergent N- and C-terminal of human PP1 isoforms and the highly conserved catalytic domain. The homology analysis of PP1 N- and C-terminal were performed using a CLUSTALW2 multiple sequence alignment. Sequence gaps are indicated with a hyphen. Red boxes in the variable C-terminal domain indicate peptides used to generate antisera in rabbits.

The antibodies used in this thesis and corresponding dilutions are indicated in Table 5.

Table 5| Antibodies and detection systems used in this dissertation. IEM, Immunoelectron microscopy; IHC, Immunohistochemistry; WB, Western blot.

Primary Antibody	Host	Dilution	Type	Supplier
Anti-PP1α	Rabbit	**IEM** 1:50 **IHC** 1:500	Polyclonal	Home-made
Anti-PP1γ2	Rabbit	**IEM** 1:500 **IHC** 1:5000	Polyclonal	Home-made
Anti-SARP2	Rabbit	**WB** 1:100 **IEM** 1:50 **IHC** 1:250	Polyclonal	Home-made
Secondary Antibody	**Host**	**Dilution**		**Supplier**
Anti-Rabbit-IgG Alexa 488	Donkey	**IHC** 1:300	-	Molecular Probes/ Invitrogen, CA 92008, USA
Secondary Detection System	**Host**	**Dilution**		**Supplier**
Protein A Gold conjugate	*S.* aureus	**IEM** 1:50	-	Home-made according to (Geuze *et al.*, 1981)

3.1.2. HUMAN SAMPLES COLLECTION

Human testis biopsies were collected as described in section 2.1.1. The human semen sample was collected by a healthy adult man donor at reproductive age by masturbation.

3.1.3. WESTERN BLOT ANALYSES

3.1.3.1. TISSUES PREPARATION

Human testis samples were homogenized, resuspended in boiling 1% SDS and sonicated 3 x 30 sec. Human sperm samples were washed in 1% PBS and then centrifuged at 600g for 5 min at room temperature (RT), the supernatant was discarded and the pellet resuspended in HB plus buffer (see appendix). Then, to separate the supernatant fraction (soluble fraction) from the pellet fraction (insoluble fraction), a centrifugation of 16000g for 20 min at 4ºC was performed. The supernatant was kept at -20ºC. The pellet was resuspended in HB plus, sonicated 3 x 15 sec at low magnification and then boiled for 5 min.

3.1.3.2. CALCULATE THE CONCENTRATION AND THE TOTAL NUMBER OF SPERMATOZOA IN SEMEN SAMPLE

Sperm concentration was evaluated according to World Health Organization guidelines (WHO, 2010). To determine the appropriate dilution, a well-mixed, undiluted preparation of liquefied semen on a glass slide under a coverslip was examined (Table 6). The semen sample was mixed and the appropriate volume of semen was added to the fixative (5 g of $NaHCO_3$ and 1 ml of 35% (v/v) formalin in 100 ml purified water). The dilution was vortexed for 10 sec and the improved Neubauer chambers were immediately filled with 10 µl of the fixed solution. The chamber was stored for approximately 5 min at RT in a humid chamber. Then, the improved Neubauer chamber (see appendix, Figure 31) was examined at 400x magnification and at least 200 spermatozoa were counted per replicate. First, the central grid (number 5) of one side of the improved Neubauer chamber was assessed (see appendix, Figure 31). The same number of rows was assessed in the other chamber. Then the concentration in spermatozoa per ml was calculated according to the formula: **C= (N/n) x (1/20) x dilution factor**. Where N is the number of spermatozoa, divided by the volume in which they were found [volume of the total number (n) of rows examined (20 nl each for grid number 5)], multiplied by the dilution factor. Finally, the total number of spermatozoa per ejaculate was calculated multiplying the sperm concentration by the semen volume (WHO, 2010).

Table 6| Semen dilutions required. Adapted from (WHO, 2010).

Spermatozoa per x400 field	Spermatozoa per x200 field	Dilution required	Semen (µl)	Fixative (µl)
>101	>401	1:20	50	950
16-100	64-400	1:5	50	200
2-15	8-60	1:2	50	50
<2	<8	1:2	50	50

3.1.3.3. SDS-PAGE

In SDS polyacrylamide gel electrophoresis (SDS-PAGE) separations were carried out using well established methods (Sambrook, 1989). The percentage and size of the gel used depended on the molecular weight of the proteins that are being separated in the gel.

Table 7 | Composition of the running and stacking gels for SDS-PAGE (*mini gels*).

Components	Running gel (10%)	Stacking gel (3.5%)
Water	4.2 ml	3.3 ml
30% Acryl/8% Bisacryl.	3.3 ml	0.6 ml
4x LGB	2.5 ml	---
5x UGB	---	1.0 ml
10% SDS	---	50 µl
10% APS	50 µl	50 µl
TEMED	5 µl	5 µl

The 10% running gel was prepared by sequentially adding the components indicated on Table 8 (APS and TEMED were added last, as they initiate the polymerizing process). The solution was pipetted down the spacer into the gel apparatus, leaving some space for the stacking gel. Then, the water was carefully added to cover the top of the gel and the gel was allowed to polymerize for 1 hr. The stacking gel was prepared according to Table 4. The water was poured out and the stacking gel was added to the apparatus; a comb was inserted and the gel was allowed to polymerize for 30 min. After the gel polymerization, the combs were removed, and the wells filled and washed with running buffer. The samples were prepared by adding to the protein sample (when appropriate, the amount of protein loaded on the gel will be described) ¼ volume of loading buffer (LB). Then, the samples were carefully applied into the wells. The gel was run for 2 hr at 100 V until bromophenol blue from the LB reached the bottom.

3.1.3.4. IMMUNOBLOTTING

For electroblotting, the tank transfer system was used as follows: 3MM blotter paper was cut to fit the transfer cassette and a nitrocellulose membrane to fit the gel size. The gel was removed from the electrophoresis apparatus and the stacking gel removed and discarded. The transfer sandwich was assembled immersed in the transfer buffer to avoid trapping air bubbles. The cassette was placed in the transfer apparatus and filled with transfer buffer. Transfer was allowed to proceed for 2 hr at 200 mA. Afterwards, the transfer cassettes were disassembled, the membrane carefully removed and allowed to air dry prior to further manipulations.

The immunodetection was performed by enhanced chemiluminescence (ECL). ECL™ (Amersham) is a light emitting non-radioactive method for the detection of immobilized antigens, conjugated directly or indirectly with horseradish peroxidase-labelled antibodies.

In order to visualize the proteins, the blots were probed with a polyclonal anti-SARP2 antibody, which recognizes only the SARP2 isoform (Figure 8). The membranes were soaked in 1xTBS for 5 min. Non-specific binding sites were blocked by immersing the membrane in 5% low fat milk in 1xTBST for 1 hr. The membrane was incubated with the primary antibody (anti-SARP2; 1:100), diluted in 3% low fat milk in 1xTBST for 2 hr with shaking. After three washes of 10 min each in 1xTBST, the membrane was incubated with the anti-rabbit secondary antibody diluted (1:5000) in 3% low fat milk in 1xTBST for 1 hr with shaking. The membrane was then washed 3 times with 1xTBST for 10 min. Subsequently, the membrane was incubated for 1 min with the ECL detection solution (a mixture of equal volumes of solution 1 and solution 2 from the ECL kit (Amersham), approximately 0.125 ml/cm^2 membrane). Inside the dark room, the membrane was gently wrapped with cling-film, eliminating all air bubbles and placed in a film cassette and an autoradiography film (XAR-5 film, KODAK) was placed on the top and the cassette was closed and the blot exposed for 10 min. The film was then removed and developed in a developing solution, washed in water and fixed in the fixing solution.

As a control, this membrane was also incubated with anti-β-tubulin antibody, to determine if the quantity of protein loaded in the gel was equal for all samples. The same membrane was washed three times during 10 min with 1xTBST, blocked, as described above, and incubated with the primary antibody (anti-β-tubulin; 1:1000), diluted in 3% low fat milk in 1xTBST for 2 hr with shaking. After this period, three washes of 10 min each in 1xTBST were done, and the membrane was then incubated with the anti-mouse secondary antibody (1:5000) in 3% low fat milk in 1xTBST for 1 hr with shaking. The membrane was then washed three times with 1xTBST for 10 min and the immunodetection was carried using ECL as described above.

3.1.4. IMMUNOELECTRON MICROSCOPY

After collection, the human testis biopsies were immediately immersed in fixative A or B (see appendix). The samples were maintained in the fixative ON, in order to achieve complete fixation. Then, the tissue was transferred into the appropriate buffer (A or B, see appendix). Fixed samples were embedded into LR White resin after dehydration in a series of graded ethanol (medium grade). LR White-filled gelatin capsules were polymerized at 50°C for 3 days (see appendix). After preparation of semi-thin sections (1 µm) and observation in the light microscope, blocks were trimmed for areas with defined stages of seminiferous tubules. Ultrathin sections of 80 nm were cut on LEICA microtome (VT1000S), collected on 100 mesh nickel grids, and thereafter coated on the back side with a 1% formvar film (support film). The grids were dried at 37°C ON prior to

immunostaining. The sections were incubated with glycine solution (0,05M glycine in TBS pH 7,4) during 15 min, in order to disable free aldehyde groups. Subsequently, sections were incubated in blocking solution (1% BSA in TBST pH 7,4) for 30 min at RT. Then, they were washed 3 times for 2 min (0,1% BSA in TBST pH 7,4). Incubation with the primary antibodies was performed on droplets with antibodies in 0.1% BSA in TBST ON at RT in a wet chamber. The grids were intensively washed on 3 series of washing solution drops (0,1% BSA in TBST pH 7,4) for 10 min. The sections were then incubated with a protein A-gold solution (1:50, 12-nm colloidal gold particles) for 90 min, at RT. Negative controls were processed in parallel by addition of TBST buffer instead of the first antibodies. The grids were rinsed on droplets of washing solution (0,1% BSA in TBST pH 7,4), 3 times, for 10 min, and subsequently contrasted with uranyl acetate for 2 min and lead citrate for 45 sec. The sections were examined using a LEO 906 electron microscope (see appendix, Figure 30) (Figure 21).

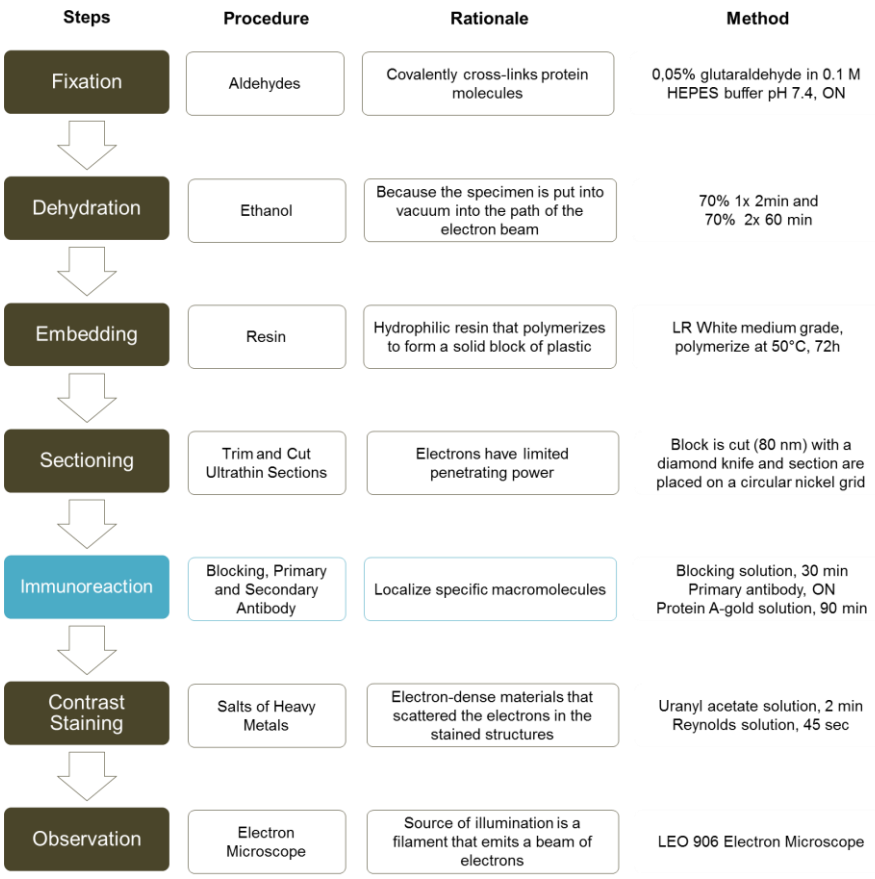

Figure 21| Immunoelectron microscopy procedure overview. Theoretically, a fixation with a lower glutaraldehyde concentration (0,05%) is more indicated to preserve antigenicity, hence more suitable for immunoelectron localizations. In order to preserve tissue antigenicity, post-fixation in osmium-tetroxide should also be avoided. Since LR White Resin has several advantages, which can be exploited for the localization of antigens, the embedding process also differs from conventional electron microscopy. The immunoreaction (blue boxes) is only used in immunoelectron microscopy. (ON, overnight; sec, seconds; min, minutes).

3.1.5. IMMUNOHISTOCHEMISTRY

Paraffin embedded human testis were cut on a microtome into sections 5 µm thick. Sections were deparaffined and rehydrated as follows: Xylol 3 x 10 min, absolute ethanol 2 x 5 min, 96% ethanol, 80% ethanol, 70% ethanol, and ddH_2O, each step for 1 x 5 min at RT. For improved retrieval of antigens and accessibility of epitopes deparaffinized and rehydrated testis sections were subjected to digestion with trypsin: slides were treated with 500µl of 0,01% trypsin (in TBS) for 10 min at 37°C, washed 3 x with improved ddH_2O for 5 min, followed by microwave treatment for 10 min at 850 W in 10 mM citrate buffer at pH 6. The samples were then washed in ddH_2O for 4 min at the microwave. Non-specific binding sites were blocked with 4% BSA for 2 h at RT and washed 3 x with TBST. After, sections were incubated with primary antibodies (Table 5) in 1% BSA in TBST ON at 4°C. On the following day, the sections were washed 3 x 5 min in TBST. Then incubated with fluorochrome-conjugated secondary antibodies (Table 5) (diluted in 1% BSA in TBST) for 2 h and washed 2 x 5 min with TBST. Negative controls were processed in parallel by adding TBST instead of the first antibodies. Nuclei were visualized with DAPI (1:200) for 5 min at RT and washed 2 x with TBST for 5 min. Finally, samples were inspected with LEICA fluorescence microscope.

3.2. RESULTS

3.2.1. SPECIFICITY OF SARP2 ANTIBODY IN HUMAN TESTIS

The presence of C-terminal isoform-specific sequence has allowed the production of antibodies that specifically recognize each SARP isoform (Figure 8). SARP2 antibody specificity in human testis and sperm was analyzed by Western blot (Figure 22).

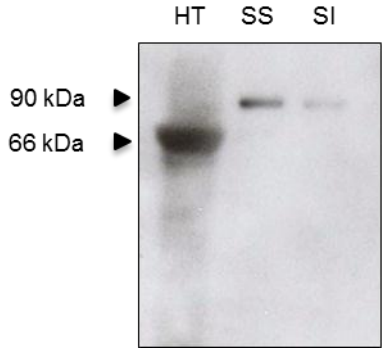

Figure 22| Characterization of anti-SARP2 antibody in human testis and sperm. A total human testis extract (HT) (~30µg) and sperm soluble (SS) and insoluble (SI) fractions ($3x10^6$ spermatozoa) were immunoblotted with anti-SARP2 isoform specific antibody.

Western blot analysis reveals specific signals at about 66 kDa in human testis and 90 kDa in human sperm. These suggest that the 66 kDa band obtained in testis represents a shorter SARP2 isoform, whereas the 90 kDa signal that appeared in sperm is a longer SARP2.

In addition, the levels of SARP2 expression in human testis are significantly higher compared with sperm soluble and insoluble fractions.

3.2.2. LOCALIZATION OF PP1 ISOFORMS AND SARP2 IN HUMAN TESTIS

TEM combined with colloidal gold particles was used for high-resolution immunolocalization of PP1α, PP1γ2 and SARP2 in human testis. A key question was to identify cell types and cellular compartments that show preferential labeling, in other words, identify structures with the highest concentrations of the molecules of interest.

3.2.2.1. LOCALIZATION OF PP1 ISOFORMS IN HUMAN TESTIS BY IEM

The data indicate that PP1α and PP1γ2 are present in different but overlapping localizations in male germ cells. They are both present in the nucleus of spermatids (Figure 23 and 24) but PP1α shows an acrosome staining in addition to nuclear staining (Figure 24). PP1 γ2 is predominant in the nucleus of elongated spermatids in different maturation stages and shows a weak immunoreactivity in the nucleus of round spermatids (Figure 23). PP1α and PP1γ2 are not observed in early stages of spermatogenesis. Interstitial cells, Sertoli cells and peritubular cells showed no immunoreactive for PP1α and PP1γ2. In all the immunoelectron experiments negative controls, without the primary antibody, were performed and no staining was observed (sections 3.2.2.1 and 3.2.2.2).

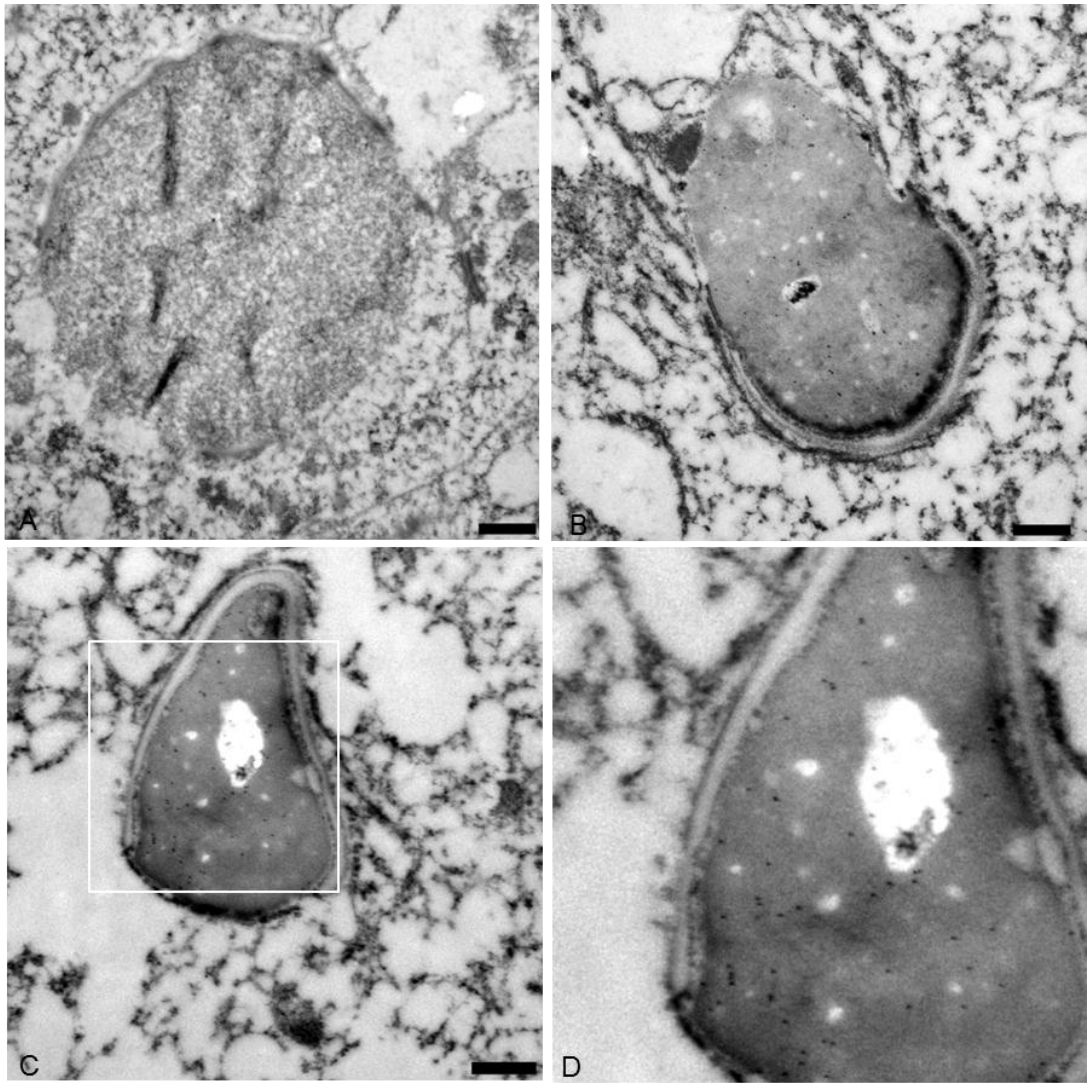

Figure 23| Electron micrographs of PP1γ2 immunoreactivity in human testis. Round spermatids shows a weak immunoreactivity in the nucleus (A). Robust immunoreactivity for PP1 γ2 is present in the nucleus of elongated spermatids in different maturation stages (B and C). D shows a higher magnification view of C. Bars represent: 500 nm. A-D: Fixative B.

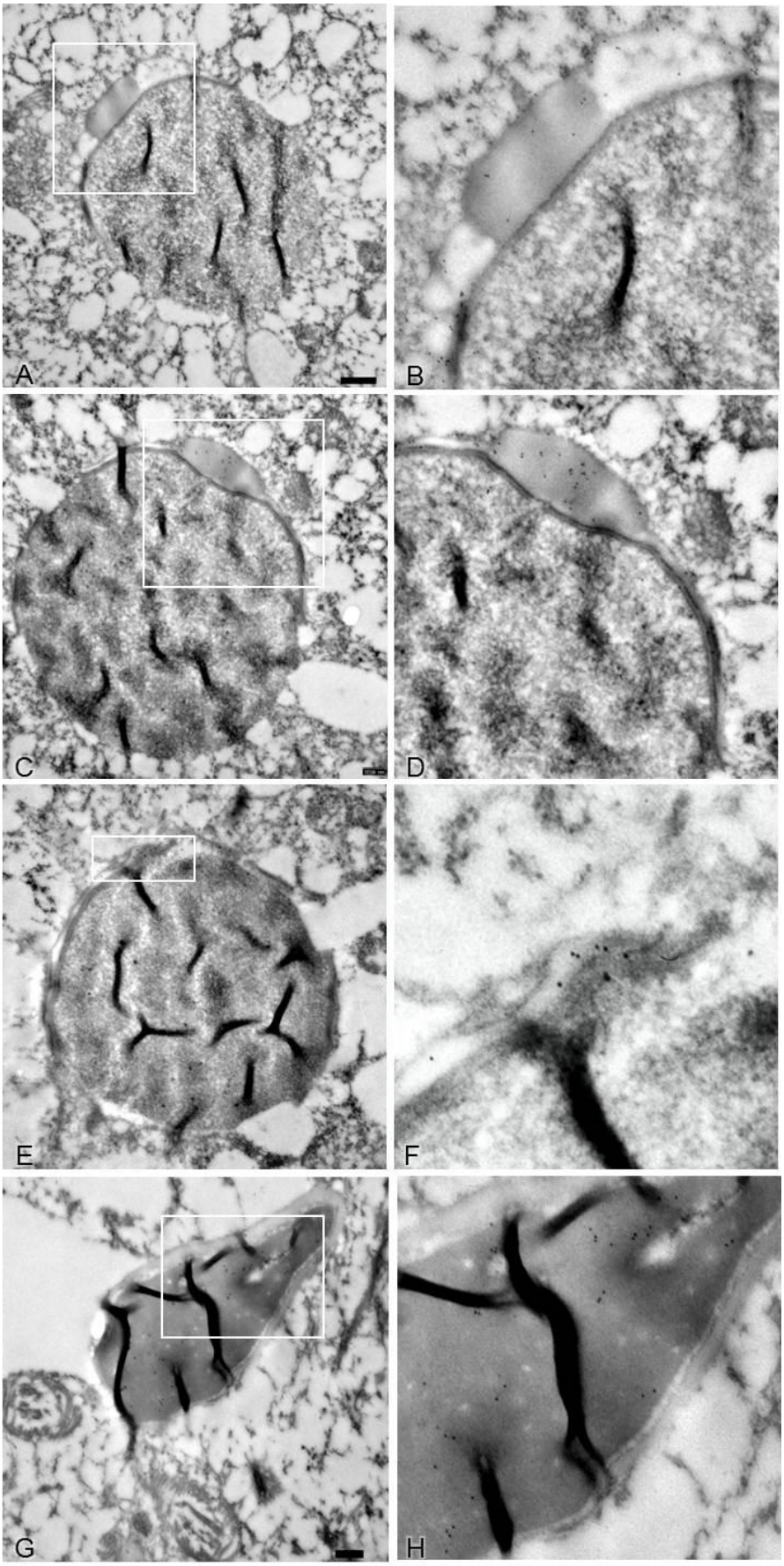
A
B
C
D
E
F
G
H

Figure 24| Electron micrographs of PP1α immunoreactivity in human testis. Round spermatid show an enrichment in the nucleus and the acrosome. At the beginning of the acrosome formation we have an enrichment of PP1α (A, C) that is not maintained until the end of maturation (G, H – higher magnification of G). B and D show a higher magnification view of the beginning of acrosome formation from A and C, respectively. Intermediate phase between round and elongated spermatid shows an enrichment of PP1α in edges of the acrosome (E). F shows a higher magnification view of the acrosome from E. In elongated spermatid the staining in the acrosome is lower than in the nucleus (G and H). Bars represent in A and E: 500 nm; G: 250 nm. A, B, C, D, G and H: Fixative B; E and F: Fixative A.

3.2.2.2. LOCALIZATION OF SARP2 IN HUMAN TESTIS

In elongated and mature spermatids SARP2 shows significant and intense staining in the nucleus which could indicate a very late state of expression in spermatogenesis, since round spermatids, and more immature germ cells, show no staining.

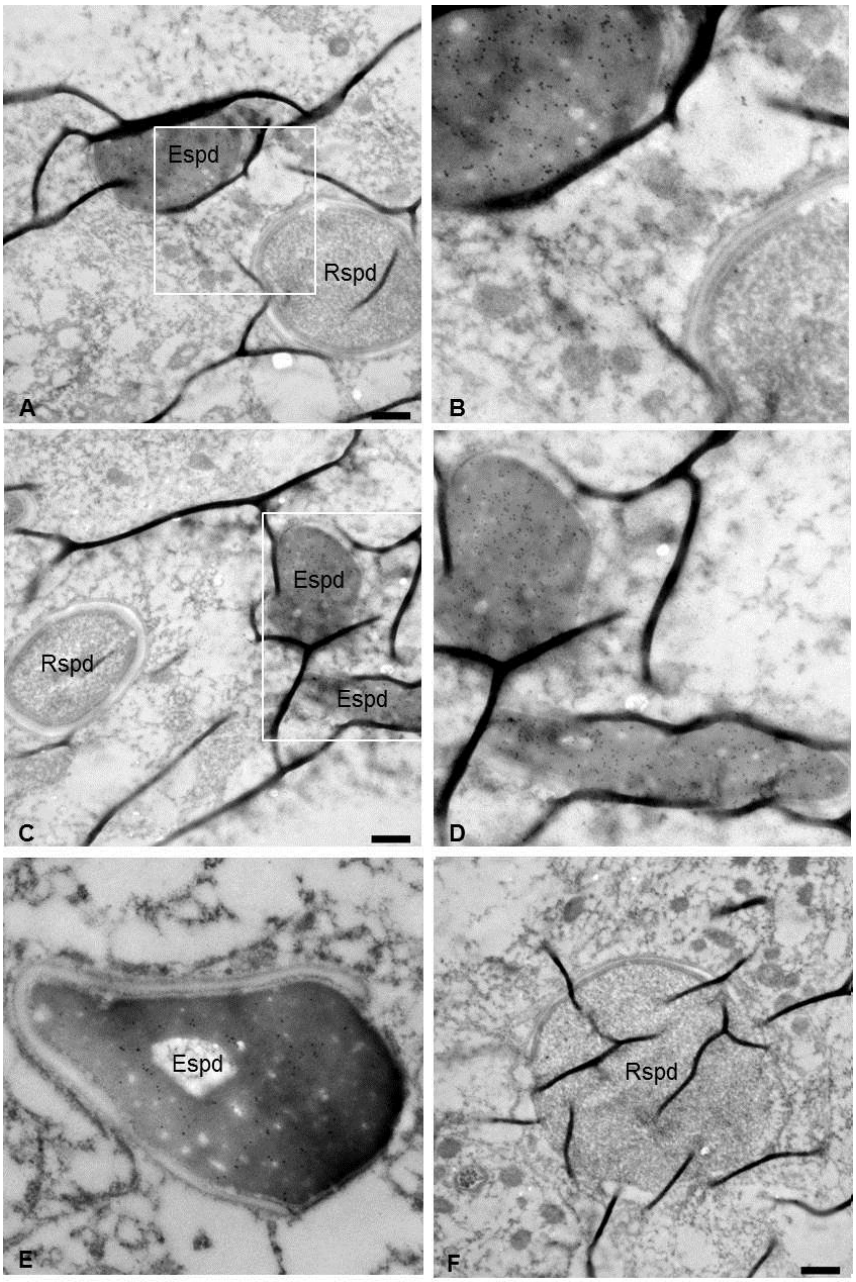

Figure 25| Electron micrographs of immunoreactivity for SARP2 in human testis. In elongated spermatids (Espd) SARP2 shows significant staining in the nucleus, while in round spermatids (Rspd) show no labeling. B and D show a higher magnification of A and C, respectively. Bars represent: 500 nm. A, B, C and D: Fixative B; E and F: Fixative A.

3.2.3. LOCALIZATION OF PP1 ISOFORMS AND SARP2 IN HUMAN TESTIS IMMUNOHISTOCHEMISTRY

The localization of PP1 isoforms and SARP2 in human testis was also performed by immunohistochemistry.

3.2.3.1. PP1 ISOFORMS

PP1α shows an intense fluorescence in round spermatids (arrowheads) and no labeling in the more mature germ cells (*).Immunofluorescence for PP1γ2 was different from that observed for PP1 α. PP1γ2 shows high labeling intensity in the seminiferous tubule adluminal part in both spermatids (arrowhead) and mature germ cells (*) (Figure 26). Autofluorescence was detected when secondary antibody was used alone.

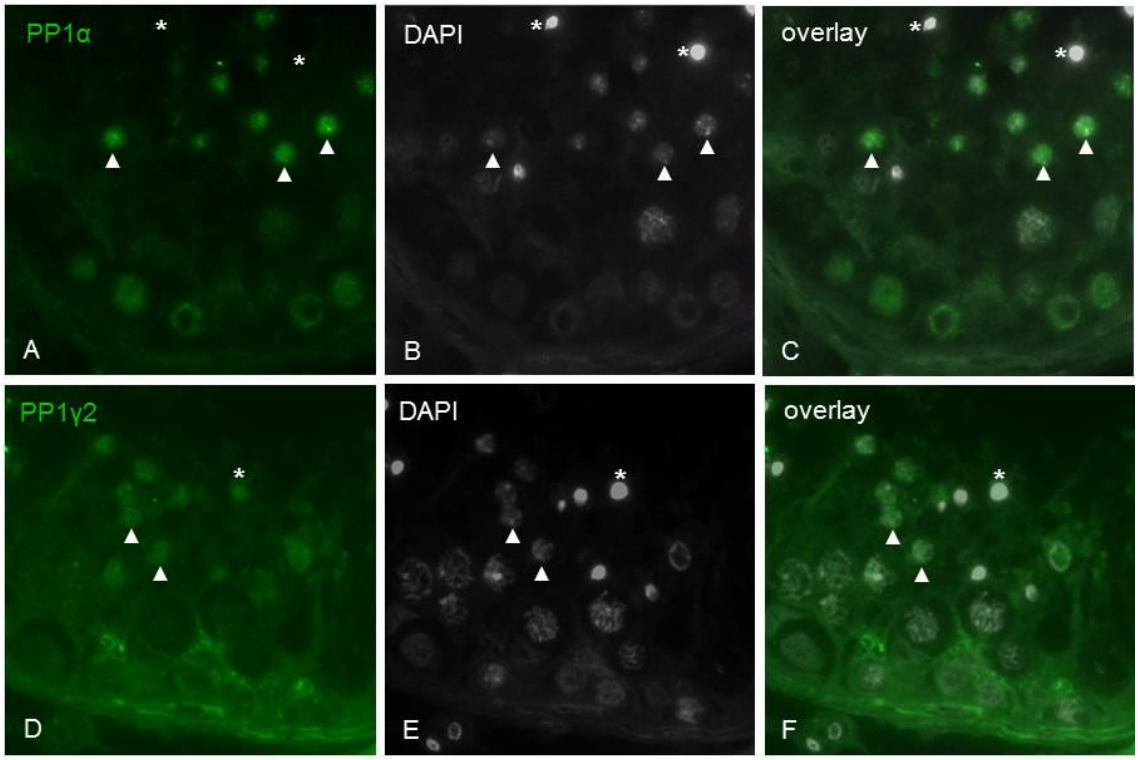

Figure 26| Immunohistochemistry detection of PP1 isoforms in seminiferous tubules of human testis. A. PP1α. B. Nuclear counterstained with DAPI for labeling the nuclei. C. Overlay of A and B. D. PP1γ2. E. Nuclear counterstained with DAPI for labeling the nuclei. F. Overlay of D and E. Note the difference in cell-type specific labeling intensities with highest abundance of PP1α in round spermatids (arrowheads) and showing no labeling in the more mature germ cells (*). PP1γ2 shows high labeling intensity in the seminiferous tubule adluminal part in both spermatids (arrowhead) and mature germ cells (*).

3.2.3.2. SARP2

SARP2 shows differences in cell-type specific labeling intensities with highest abundance of in late stages of spermatogenesis (arrows) (Figure 27). Autofluorescence was detected when secondary antibody was used alone.

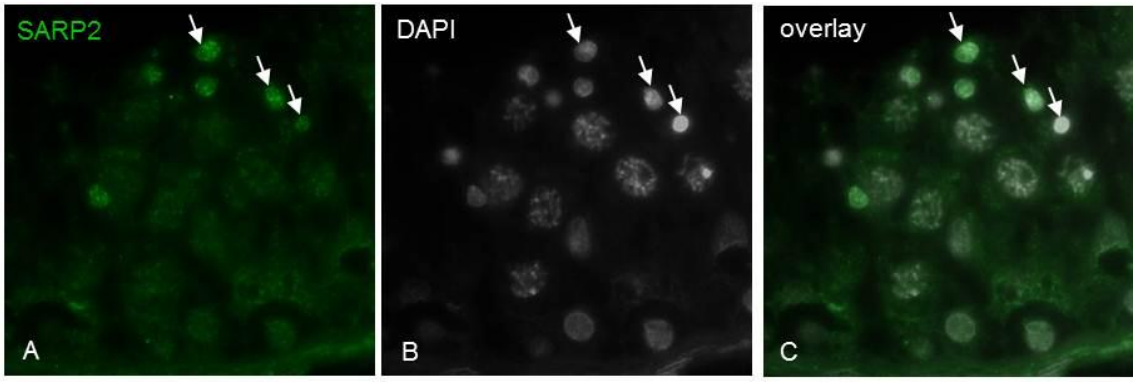

Figure 27| Immunohistochemistry detection of SARP2 in seminiferous tubules of human testis. A. SARP2 B. Nuclear counterstained with DAPI for labeling the nuclei. C. Overlay of A and B.

3.3. DISCUSSION

In this study, we incubate thin sections of human testis with specific primary antibodies (PP1 isoforms and SARP2), and then with secondary antibodies attached to colloidal gold particles, which are heavy metal based and provide good visualizing by TEM. The gold particles are electron-dense and can be seen as a black dot in the electron microscope. Since the scattered electrons are lost from the beam, the dense regions of the specimen show up as areas of reduced electron flux, which look dark. The spatial distribution of the particles in thin sections of the tissues was based on the qualitative inspection of TEM images. More rigorous examination requires quantitative approaches, which provide a statistically robust format for quantitative comparisons over multiple compartments. The first step was to assess if the labeling pattern of the different proteins in study was distinct, then if the distribution of particles was random or if there was a preferential localization and finally, if there were changes in distribution patterns between germ cell types.

The ultrastructure analyses showed that tissue was well preserved, what reinforces our immunolocalizations. The preservation of structural detail of tissue for TEM involves different steps: fixation, dehydration and embedding. All these procedures can have deleterious effects on the antigen resulting in the loss of antibody binding. Therefore, in order to successfully immunolocalize an antigen, a compromise between the preservation of ultrastructural detail and the retaining of antigenicity had to be reached.

We analyzed and compared tissue and antigenicity preservation efficiency of two fixatives on testis ultrathin sections. A fixative containing until 0.5% glutaraldehyde is generally suitable for a wide variety of antigens (Oliver, 1994). Our results indicate that an optimal preservation of human testis ultrastructure can be achieved with both fixatives used and the antibodies labeling patterns are not influenced by the fixative used (A or B).

For ultrastructural immunolocalisation of antigens, three methods have been developed: pre-embedding immunolabelling, post-embedding immunolabelling and cryo-immunolabelling (Table 8). With pre-embedding immunolabelling the tissue is fixed, followed by the immunolabelling procedure before dehydration, embedding and sectioning. For post-embedding immunolabelling, the immunolabelling takes place only after fixation, dehydration, embedding and sectioning. The third of these methods, cryo-immunolabelling, is considered to be the method giving superior results when compared to the first two. The antigen is preserved best during cryo-treatment since the antigen is not exposed to any of the treatments before the immunolabelling step takes place (Bendayan *et al.*, 1987) (Table 8).

Table 8| Methods for ultrastructural immunolocalisation of antigens: advantages and disadvantages.

Method	Advantages	Disadvantages
Pre-embedding immunolabelling	Antigen not exposed to the organic solvents;	Low antibody penetration; Irregular labeling; Need for permeabilization procedures; Loss of ultrastructure detail due to permeabilization;
Post-embedding immunolabelling	No permeabilization step required;	Changes in the antigen's structure; Decrease binding of the antibody;
Cryo-immunolabelling	Best antigen preservation; Sections fully penetrable to antibodies;	Antigen may be extracted during the immunolabelling due to weak fixation and absence of embedding;

For this study, since cryo-immunolabelling was not available post-embedding immunolabelling was chosen, since pre-embedding immunolabelling is more disadvantageous for quantifying the immunolabelling due to possible non-homogenous antibody penetration. However, the manipulation of the tissue during its processing for post-embedding immunolabelling can result in modifications of tissue components. Proteins are extremely prone to these modifications and, as a consequence, the binding of antibody to antigens can be changed or even lost. For post-embedding immunolabelling procedures, a hydrophilic resin was used (LR White) since it gives better results than the epoxy-based hydrophobic resins. There are a number of factors responsible for the better immunolabelling with the hydrophilic resins: (1) LR White is compatible with about 12% by volume of water so that partial dehydration with an organic solvent is possible; (2) LR White is less lipophilic than epoxides and therefore less likely to disrupt ultrastructure by extraction of, especially, lipids since post-fixation with osmium tetroxide was omitted; (3) In contrast with epoxies, LR White does not form covalent bonds with biological material during the polymerisation procedure. The reactive epoxy groups have a great tendency to react with hydroxyl and amino groups, which are chemical side-groups present in proteins and nucleic acids. Therefore, the bio-molecules will be part of the polymer network. LR White polymerizes by free radical chain polymerization. These free radicals react with double bonds of the acrylic monomer and have no affinity for proteins and nucleic acids. Thus, bio-molecules are not incorporated into the polymer network (Brorson, 1998).

With post-embedding immunolabelling, non-specific binding of the antibodies can occur to either the resin itself, non-specific reactive sites on the tissue or to bio-molecules. To reduce non-specific

labeling to the resin and to the tissue, a blocking agent was used (BSA) to prevent the reactive sites from binding to the antibody. Furthermore, the free aldehyde groups that remained after fixation with glutaraldehyde can react with the antibodies resulting in non-specific labeling. In order to block these free groups, glycine, a small molecular weight compound containing an amino acid group, was used. Unlike epoxy resins, the resin used (LR White) is a hydrophilic resin displaying a low attraction for other hydrophilic substances such as antibodies.

One of the major obstacles with post-embedding immunolabelling is that immunolabelling arises from antigen only exposed on the surface of the section. Therefore, high concentrations of antibody are required normally. To achieve specific immunolabelling for PP1γ2 we had to test two different antibody dilutions (1:50 and 1:500). No specific immunolabelling was achieved for the 1:50 dilution and so we use the 1:500 dilution.

3.3.1.1. PP1 ISOFORMS IN HUMAN TESTIS

PP1 achieves the specificity towards the substrates not only by the diversity of the binding partners but also through different catalytic subunits. Most studies have not directly addressed the significance of the different isoforms and simply refer the phosphatase as PP1c. But it is well established that they have distinct tissue specificity and subcellular localization (da Cruz e Silva *et al.*, 1995; Ouimet *et al.*, 1995; Andreassen *et al.*, 1998; Strack *et al.*, 1999). Some studies have shown different localization patterns of PP1 isoforms and demonstrate that some PIPs discriminate among the isoforms (Terry-Lorenzo *et al.*, 2002).

Different distributions of PP1 isoforms could indicate that these phosphatase isoforms dephosphorylate distinct sets of substrates and, therefore, are involved in regulating different aspects of testis and sperm function, such as spermatogenesis, acrosome biogenesis, sperm differentiation, maturation and function. While previous reports (Chakrabarti *et al.*, 2007) have shown the PP1 distribution in mouse testis, its distribution within specific cell types in human testis relative to other PP1 isoforms was unknown.

Chakrabarti and colleagues (Chakrabarti *et al.*, 2007) determine the expression patterns of PP1 isoforms in mice testes. PP1γ2 was prominently expressed in round spermatids as well as in elongating spermatids and testicular spermatozoa, whereas its expression was weak or absent in spermatogonia, pachytene spermatocytes, and interstitial cells. In contrast, a high level of PP1γ1 expression was observed in interstitial cells, whereas much weaker expression was observed in

germ cells. PP1α, was predominant in spermatogonia, pachytene spermatocytes, and interstitial cells.

In this study we have reported, for the first time, the expression patterns of PP1γ2, the predominant PP1 isoform in male germ cells, and PP1α in human testis. Our immunoelectron microscopy results show that PP1γ2 is present in abundance in late stages of germ cell maturation, whereas for the most part, PP1α expression is present in spermatids nucleus and during the acrosome formation.

In order to confirm our immunoelectron microscope results we performed immunohistochemistry analyses. Fluorescence patterns also showed a distinct expression of the different PP1 isoforms in human testis sections. PP1γ2 immunohistochemistry was predominant in the seminiferous tubule adluminal part in both spermatids and mature germ cells. PP1α is more expressed in round spermatids without showing an intense labeling in the more mature germ cells. However, immunohistochemistry analyses has to be repeated due to poor tissue preservation and the high presence of background.

Our results are consistent with previous studies that determine the expression of PP1 isoforms in testis from mice of increasing postnatal ages and, showed an increase in PP1γ2 expression and a decrease in PP1γ1 and PP1α with age (Chakrabarti *et al.*, 2007). The different ages mark the approximate times at which distinct germ cell is produced in the testis, for instance, until day 8, spermatogonia are the only germ cells in the seminiferous tubules and spermatid formation occurs at day 18. The increase in PP1γ2 expression is consistent with spermatids formation.

Targeted deletion of *Ppp1cc* gene leads to sterility in males due to a combination of gross structural defects in developing spermatids, resulting in apoptosis and faulty spermiation (Varmuza *et al.*, 1999). Electron microscopy studies in *Ppp1cc-null* male mices mutants also revealed major chromatin condensation defects in elongating spermatids (Forgione *et al.*, 2010). These facts are consistent with PP1γ2 immunolocalization that demonstrates high expression level in postmeiotic male germ cells (spermatids).

3.3.1.2. SARP2 IN HUMAN TESTIS

A number of PIPs have been detected in somatic cells and considerable progress has been made in defining the function of these proteins and how they regulate PP1 (Parrish *et al.*, 2006). However, our understanding on the regulation of PP1 in male germ cells is limited. In order to identify and define the properties of the protein regulators of human testis PP1, YTH screens of a human testis cDNA libraries, using PP1γ1 and PP1γ2 as baits were performed. One of the identified PIPs was

SARP. SARP2 (92–94 kDa) is ubiquitously expressed with high levels in testis and sperm, where it interacts with both PP1γ1 and PP1γ2. However, little is known about SARP2 exact localization and functions in human testis and spermatozoa.

Western blot analysis was performed to show SARP2 antibody specificity, revealing specific signals at about 66 kDa in human testis and 90 kDa in human sperm. These suggest that the 66 kDa band obtained in testis represents a shorter SARP2 isoform, whereas the 90 kDa signal that appeared in sperm is a longer SARP2. For further studies, a Northern blot analyses in several human tissues should allow us to detect a different size transcript in testis. Some proteins where transcription can be initiated at different transcription start sites have also been reported. This pattern is particularly common in testis: ACE-T, testis angiotensin-converting enzyme (Zhou *et al.*, 1995); DDX3Y, DEAD-box Y (DBY) RNA helicase (Jaroszynski *et al.*, 2010); GnRH, gonadotropin-releasing hormone (Dong *et al.*, 1996); MTHFR, methylenetetrahydrofolate reductase (Tran *et al.*, 2002); Cyp19, aromatase cytochrome P450-encoding gene (Fürbass *et al.*, 1997); GAT1, GABA transporter 1 (Jin *et al.*, 2001), are some examples. In SARP2, a Kozak sequence suggests that the ATG, originating a transcript of about 66 kDa, is likely to initiate translation. To test this hypothesis, a five prime rapid amplification of cDNA end (5' RACE) can be used to determine SARP2 transcriptional starting sites in testis and the products can be further confirmed by DNA sequencing.

Our study revealed that SARP2 exhibits a tissue, cell type, and spermatogenic stage specificity. SARP2 is more abundant in testis, and within the testis it is expressed only in post-meiotic haploid spermatids, mainly in mid/late stages of elongated spermatids. Given the unique expression pattern of SARP2, we propose that it might play a significant role in sperm differention and/or function. SARP2 high enrichment in the nucleus of the elongating spermatids is consistent with the putative nuclear localization signal at the N-terminus.

Additionally, SARP2 shows the same localization in human testis as the PP1 testis/sperm-specific isoform, PP1γ2. Further studies are needed to identify the role of PP1γ2/SARP2 holoenzyme in male reproductive function.

Similarly to SARP2, ACE-T, a testis-specific androgen-dependent ACE isozyme, is found in post-meiotic spermatids (Pauls *et al.*, 2003). Male mice homozygous for a disrupted ACE gene are almost infertile. Despite showing normal testis histology and sperm parameters, the oviduct transport and zona pellucida binding is impaired (Krege *et al.*, 1995). It is estimated that the unique N-terminal of ACE-T possesses specific binding properties (Kessler *et al.*, 2000).

Another protein that shows some similarities with SARP2 is Atce1. Tissue distribution of Atce1 transcripts revealed that it is restricted to late haploid round spermatids and to elongating spermatids. Atce1 was identified in an YTH screen when searching for genes that are significantly upregulated during spermiogenesis (Takayuki *et al.*, 2001). This protein contains a basic domain followed by a leucine zipper motif (bZIP domain). The six C-terminal amino acids of the basic domain constitute a putative nuclear localization signal (Stelzer *et al.*, 2002). This peptide shows significant homology to the CREB subfamily.

SARP2 possess a putative leucine-zipper motif near the C-terminus suggesting that they may function as transcription factor or cofactor. Several studies have indicated that PP1 interacts with proteins that modulate transcription. An alignment of the SARP2 C-terminal region with the leucine-zipper regions of representative members of transcription factor families reveals that SARP2 C-terminus is related to the KE2 family of leucine-zipper proteins, which encompasses proteins involved in tubulin folding. Nevertheless, the specific binding of SARP2 to mammalian DNA supports a role for SARP2 as transcription factor or cofactor and suggests that PP1 may participate in the regulation of transcription in testis via SARP2 (Browne *et al.*, 2007).

During spermiogenesis, many testis-specific proteins are required for the drastic changes that occur. Toward the end of spermiogenesis, chromatin begins to condense by the replacement of histones with protamines, the nucleosomal structure disappears and the transcriptional activity ceases (Sassone-Corsi, 2002). Therefore, testis-specific gene expression occurs in germ cells before chromatin condensation. Male germ-cell differentiation requires spermatogenic stage- and cell-specific gene expression. Testis has specialized transcription mechanisms such as, upregulated expression of the TATA-binding protein (TBP) family and its associated cofactor and cAMP-response-element modulator (CREM), a transcription factor responsive to the cAMP signal transduction pathway, responsible for the expression of key testis specific genes. As spermatocytes complete the meiotic division and enter the haploid phase, a prominent switch occurs from inhibitory to activating isoforms of CREM (De Cesare et al., 2000).

4. FINAL CONCLUSIONS

Immunoelectron microscopy combines the specificity and sensitivity of immunological methods with the high structural resolution of electron microscopy, providing an *in situ* correlation and visualization of antigen-binding sites and ultrastructure (Schwarz *et al.*, 2001). Immunoelectron microscopy has a number of advantages over light-based methods. First, it provides a resolution higher than conventional microscopy (2 nm vs. 200 nm). Second, it provides unequalled amounts of morphological and spatial information by allowing visualization of the structural context onto which labeling compounds are mapped. Last, it allows fixation methods that provide good structural preservation (Mayhew *et al.*, 2008).

Our results from immunoelectron microscopy suggest unique male germ cell developmental functions for each PP1 isoform. PP1γ2, with its distribution in postmeiotic germ cells mainly in elongated spermatids and being the only isoform detected in sperm, is more likely to play a role in sperm morphogenesis and sperm function. PP1α is expressed in spermatids nucleus and during the acrosome formation being likely to play a role in, for instance, acrosome formation.

To confirm the cellular localizations, mRNA and protein expression analyses of PP1 isoforms in isolated germ cells by Northern and Western blot, respectively, should be performed. For the subcellular localizations, Western blot analyses of PP1 isoforms in different fractions (cytoplasmic, plasma membrane, nuclear and cytoskeleton) from human testis must be done.

In human, spermiogenesis represents a period of differentiation of about 16 days, and thus targeting these cells would represent a contraceptive approach with a relatively rapid onset and recovery. These cells express a high number of very specific transcripts and many of these are functional and/or essential for sperm differentiation and function (Ivell *et al.*, 2004). In this context, SARP2 could represent a good target for male contraception, since it is a highly abundant SARP isoform in testis and is expressed only in the post-meiotic elongated spermatids. Additionally, SARP2, a PIP, shows the same localization in human testis as PP1γ2 (testis/sperm specific PP1 isoform).

Further studies are needed to identify the role of SARP2 in testis, for instance, developmental Northern and Western blots to determine, respectively, the transcription and expression of SARP2 in testis from mice of increasing postnatal ages at which distinct germ cell populations are produced (Bellvé, 1993). We can also examine if the levels of SARP2 in *Ppp1cc*-null testis are reduced, since males have seminiferous tubules that are virtually devoid of condensing and elongating spermatids (Varmuza *et al.*, 1999). An option to test whether SARP has specific roles in sperm differentiation and/or function is to make a specific knockout of the SARP2 isoform, that will allow us to verify if the mice have normal testis histology, but impaired sperm differentiation and/or function.

Another potential contraceptive approach proposed is the targeting epididymis mechanisms. In order to enable the development of epididymal contraceptives, studies to reveal details in the epididymal sperm maturation are urgently needed. The mechanisms by which human epididymis epithelium secretes the epididymosomes and the secreted proteins are transferred to spermatozoa should be studied. Additionally, no more than 10% of all proteins present in the epididymal fluid have been identified and there is no evidence of specific roles for the majority of the epididymal proteins already identified (Dacheux *et al.*, 2009). Contraceptives acting by a post-testicular action should be designed to take advantage of the epididymis physiology. To that end, we propose approaches such as (1) interfering with the unconventional epididymal epithelial secretion (apocrine secretion) to modify the composition of luminal fluid so that the concentrations of the factors needed for sperm maturation are reduced or (2) directly targeting the spermatozoa with inhibitors of sperm function, for example, blocking sperm motility (Fardilha *et al.*, 2011). A potential difficulty is that the epididymis, as a somatic mesonephric derivative, exhibits less tissue specificity compared to the spermiogenesis specific transcripts.

In conclusion, PP1γ2 and SARP2, a PIP, have the same pattern of localization being the complex a putative good target for male contraception or male infertility treatment in the future.

REFERENCES

Alessi, D., L. K. Macdougall, et al. (1992). "The control of protein phosphatase-1 by targetting subunits." European Journal of Biochemistry **210**(3): 1023-1035.

Allen, P. B., Y.-G. Kwon, et al. (1998). "Isolation and Characterization of PNUTS, a Putative Protein Phosphatase 1 Nuclear Targeting Subunit." Journal of Biological Chemistry **273**(7): 4089-4095.

Amann, R. P. (1981). "A Critical Review of Methods for Evaluation of Spermatogenesis from Seminal Characteristics." J Androl **2**(1): 37-58.

Amann, R. P. (2008). "The Cycle of the Seminiferous Epithelium in Humans: A Need to Revisit?" J Androl **29**(5): 469-487.

Anderson, K., V. Nisenblat, et al. (2010). "Lifestyle factors in people seeking infertility treatment – A review." Australian and New Zealand Journal of Obstetrics and Gynaecology **50**(1): 8-20.

Ando, H., A. Mizutani, et al. (2006). "IRBIT suppresses IP3 receptor activity by competing with IP3 for the common binding site on the IP3 receptor." Mol Cell **22**(6): 795-806.

Andreassen, P. R., F. B. Lacroix, et al. (1998). "Differential Subcellular Localization of Protein Phosphatase-1 α, γ1, and δ Isoforms during Both Interphase and Mitosis in Mammalian Cells." The Journal of Cell Biology **141**(5): 1207-1215.

Aoyama, H., Y. Ikeda, et al. (2011). "Isoform-specific roles of protein phosphatase 1 catalytic subunits in sarcoplasmic reticulum-mediated Ca2+ cycling." Cardiovascular Research **89**(1): 79-88.

Aponte, P. M., M. P. A. Van Bragt, et al. (2005). "Spermatogonial stem cells: characteristics and experimental possibilities." APMIS **113**(11-12): 727-742.

Aumüller, G., B. Wilhelm, et al. (1999). "Apocrine secretion -- Fact or artifact?" Annals of Anatomy - Anatomischer Anzeiger **181**(5): 437-446.

Ayllon, V., X. Cayla, et al. (2002). "The anti-apoptotic molecules Bcl-xL and Bcl-w target protein phosphatase 1alpha to Bad." Eur J Immunol **32**(7): 1847-1855.

Ayllón, V., X. Cayla, et al. (2001). "Bcl-2 Targets Protein Phosphatase 1α to Bad." The Journal of Immunology **166**(12): 7345-7352.

Barford, D., A. K. Das, et al. (1998). "The Structure and Mechanism of Protein Phosphatases: Insights into Catalysis and Regulation." Annual Review of Biophysics and Biomolecular Structure **27**(1): 133-164.

Bellvé, A. R. (1993). "Purification, culture, and fractionation of spermatogenic cells." Methods Enzymol. **225**: 84-113.

Bendayan, M., A. Nanci, et al. (1987). "Effect of tissue processing on colloidal gold cytochemistry." Journal of Histochemistry & Cytochemistry **35**(9): 983-996.

Bennett, D. and L. Alphey (2002). "PP1 binds Sara and negatively regulates Dpp signaling in Drosophila melanogaster." Nat Genet **31**(4): 419-423.

Benton, L., L.-X. Shan, et al. (1995). "Differentiation of adult Leydig cells." The Journal of Steroid Biochemistry and Molecular Biology **53**(1-6): 61-68.

Bollen, M., W. Peti, et al. (2010). "The extended PP1 toolkit: designed to create specificity." Trends in biochemical sciences **35**(8): 450-458.

Brendel, C., M. Rehbein, et al. (2004). "Characterization of Staufen 1 ribonucleoprotein complexes." Biochem J **384**(Pt 2): 239-246.

Brorson, S. H. (1998). "Antigen detection on resin sections and methods for improving the immunogold labeling by manipulating the resin.

." Histol Histopathol. **13(1)**: 275-281.

Browne, G. J., M. Fardilha, et al. (2007). "SARP, a new alternatively spliced protein phosphatase 1 and DNA interacting protein." Biochem J **402**(1): 187-196.

Browne, G. J., M. Fardilha, et al. (2007). "SARP, a new alternatively spliced protein phosphatase 1 and DNA interacting protein." Biochem J **402**(1): 187-196.

Brush, M. H., D. C. Weiser, et al. (2003). "Growth Arrest and DNA Damage-Inducible Protein GADD34 Targets Protein Phosphatase 1{alpha} to the Endoplasmic Reticulum and Promotes Dephosphorylation of the {alpha} Subunit of Eukaryotic Translation Initiation Factor 2." Mol. Cell. Biol. **23**(4): 1292-1303.

Cao, W., S. N. Mattagajasingh, et al. (2002). "TIMAP, a novel CAAX box protein regulated by TGF-beta 1 and expressed in endothelial cells." Am J Physiol Cell Physiol **283**(1): C327-337.

Ceulemans, H. and M. Bollen (2004). "Functional diversity of protein phosphatase-1, a cellular economizer and reset button." Physiol Rev **84**(1): 1-39.

Chakrabarti, R., D. Kline, et al. (2007). "Analysis of Ppp1cc-Null Mice Suggests a Role for PP1gamma2 in Sperm Morphogenesis." Biology of Reproduction **76**(6): 992-1001.

Chen, S., C. T. Kesler, et al. (2009). "Androgen Receptor Phosphorylation and Activity Are Regulated by an Association with Protein Phosphatase 1." Journal of Biological Chemistry **284**(38): 25576-25584.

Cheng, L., S. Pilder, et al. (2009). "PP1γ2 and PPP1R11 Are Parts of a Multimeric Complex in Developing Testicular Germ Cells in which their Steady State Levels Are Reciprocally Related." PLoS ONE **4**(3): e4861.

Christensen, A. K. and K. C. Peacock (1980). "Increase in Leydig Cell Number in Testes of Adult Rats Treated Chronically with an Excess of Human Chorionic Gonadotropin." Biology of Reproduction **22**(2): 383-391.

Chun, Y. S., J. W. Park, et al. (1999). "Role of the 78-kDa glucose-regulated protein as an activity modulator of protein phosphatase1gamma2." Biochem Biophys Res Commun **259**(2): 300-304.

Clermont, Y. (1963). "The cycle of the seminiferous epithelium in man." Am J Anat. **112**: 35-51.

Clermont, Y. and B. Perey (1957). "Quantitative study of the cell population of the seminiferous tubules in immature rats." American Journal of Anatomy **100**(2): 241-267.

Cohen, P. (2002). "Protein phosphatase 1--targeted in many directions." J Cell Sci **115**: 241 - 256.

Cohen, P. T. W. (1997). "Novel protein serine/threonine phosphatases: Variety is the spice of life." Trends in biochemical sciences **22**(7): 245-251.

Cooke, H. J. and P. T. K. Saunders (2002). "Mouse models of male infertility." Nat Rev Genet **3**(10): 790-801.

Csortos, C., I. Czikora, et al. (2008). "TIMAP is a positive regulator of pulmonary endothelial barrier function." Am J Physiol Lung Cell Mol Physiol **295**(3): L440-450.

da Cruz e Silva, E., C. Fox, et al. (1995). "Differential expression of protein phosphatase 1 isoforms in mammalian brain." J. Neurosci. **15**(5): 3375-3389.

Dacheux, J.-L., C. Belleannée, et al. (2009). "Mammalian epididymal proteome." Molecular and Cellular Endocrinology **306**(1-2): 45-50.

Dacheux, J.-L., S. Castella, et al. (2005). "Epididymal cell secretory activities and the role of proteins in boar sperm maturation." Theriogenology **63**(2): 319-341.

de-Kretser, D. M. and J. B. Kerr (1994). The cytology of the testis In: Knobil E, Neill JD. The Physiology of Reproduction. New York, Raven.

Dong, K.-W., P. Duval, et al. (1996). "Multiple transcription start sites for the GnRH gene in rhesus and cynomolgus monkeys: a non-human primate model for studying GnRH gene regulation." Molecular and Cellular Endocrinology **117**(2): 121-130.

Dubé, E., P. T. K. Chan, et al. (2007). "Gene Expression Profiling and Its Relevance to the Blood-Epididymal Barrier in the Human Epididymis." Biology of Reproduction **76**(6): 1034-1044.

Ehmcke, J. and S. Schlatt (2006a). "A revised model for spermatogonial expansion in man: lessons from non-human primates." Reproduction **132**(5): 673-680.

Ehmcke, J., J. Wistuba, et al. (2006b). "Spermatogonial stem cells: questions, models and perspectives." Human Reproduction Update **12**(3): 275-282.

Enz, R. (2002). "The metabotropic glutamate receptor mGluR7b binds to the catalytic γ-subunit of protein phosphatase 1." Journal of Neurochemistry **81**(5): 1130-1140.

Eto, M. (2009). "Regulation of Cellular Protein Phosphatase-1 (PP1) by Phosphorylation of the CPI-17 Family, C-kinase-activated PP1 Inhibitors." Journal of Biological Chemistry **284**(51): 35273-35277.

Eynde, A. V., W. Stefaan, et al. (1995). "Molecular Cloning of NIPP-1, a Nuclear Inhibitor of Protein Phosphatase-1, Reveals Homology with Polypeptides Involved in RNA Processing." Journal of Biological Chemistry **270**(47): 28068-28074.

Fardilha, M., S. L. C. Esteves, et al. (2011). "Protein Phospatase 1 Complexes Modulate Sperm Motility and Present Novel Targets for Male Infertility." Molecular Human Reproduction.

Fardilha, M., S. L. C. Esteves, et al. (2010). "The Physiological Relevance of Protein Phosphatase 1 and its Interacting Proteins to Health and Disease." Current Medicinal Chemistry **17**(33).

Fardilha, M., S. L. C. Esteves, et al. (2011). "Identification of the human testis protein phosphatase 1 interactome." Biochemical Pharmacology **In Press, Corrected Proof**.

Fardilha, M., W. Wu, et al. (2004). "Alternatively spliced protein variants as potential therapeutic targets for male infertility and contraception." Ann N Y Acad Sci **1030**: 468-478.

Fardilha, M., W. Wu, et al. (2004). "Alternatively Spliced Protein Variants as Potential Therapeutic Targets for Male Infertility and Contraception." Annals of the New York Academy of Sciences **1030**(1): 468-478.

Flickinger, C. J., S. S. Howards, et al. (1978). "Ultrastructural differences in efferent ducts and several regions of the epididymis of the hamster." Am. J. Anat. **152**: 557-586.

Flores-Delgado, G., C. W. Y. Liu, et al. (2007). "A Limited Screen for Protein Interactions Reveals New Roles for Protein Phosphatase 1 in Cell Cycle Control and Apoptosis." Journal of Proteome Research **6**(3): 1165-1175.

Forgione, N., A. W. Vogl, et al. (2010). "Loss of protein phosphatase 1cγ (PPP1CC) leads to impaired spermatogenesis associated with defects in chromatin condensation and acrosome development: an ultrastructural analysis." Reproduction **139**(6): 1021-1029.

Frenette, G., C. Lessard, et al. (2002). "Selected Proteins of "Prostasome-Like Particles" from Epididymal Cauda Fluid Are Transferred to Epididymal Caput Spermatozoa in Bull." Biology of Reproduction **67**(1): 308-313.

Fürbass, R., C. Kalbe, et al. (1997). "Tissue-Specific Expression of the Bovine Aromatase-Encoding Gene Uses Multiple Transcriptional Start Sites and Alternative First Exons." Endocrinology **138**(7): 2813-2819.

Gallego, M., H. Kang, et al. (2006). "Protein phosphatase 1 regulates the stability of the circadian protein PER2." Biochem J.(Pt 1): . **399**: 169-175.

Gallego, M. and D. M. Virshup (2005). "Protein serine/threonine phosphatases: life, death, and sleeping." Current Opinion in Cell Biology **17**(2): 197-202.

Gatti, J.-L., S. Métayer, et al. (2005). "Identification, Proteomic Profiling, and Origin of Ram Epididymal Fluid Exosome-Like Vesicles." Biology of Reproduction **72**(6): 1452-1465.

Geuze, H. J., J. W. Slot, et al. (1981). "Use of colloidal gold particles in double-labeling immunoelectron microscopy of ultrathin frozen tissue sections." The Journal of Cell Biology **89**(3): 653-665.

Gould, S. F. and M. H. Bernstein (1979). "Fine Structure of Fetal Human Testis and Epididymis." Systems Biology in Reproductive Medicine **2**(2): 93-99.

Gunawardena, S. R., B. L. Ruis, et al. (2008). "NOM1 Targets Protein Phosphatase I to the Nucleolus." Journal of Biological Chemistry **283**(1): 398-404.

Heller, C. and Y. Clermont (1964). "KINETICS OF THE GERMINAL EPITHELIUM IN MAN." Recent Prog Horm Res **20**: 545-575.

Helps, N. R., H. M. Barker, et al. (1995). "Protein phosphatase 1 interacts with p53BP2, a protein which binds to the tumour suppressor p53." FEBS Letters **377**(3): 295-300.

Hendrickx, A., M. Beullens, et al. (2009). "Docking Motif-Guided Mapping of the Interactome of Protein Phosphatase-1." Chemistry & biology **16**(4): 365-371.

Hermanson, O., K. Jepsen, et al. (2002). "N-CoR controls differentiation of neural stem cells into astrocytes." Nature **419**(6910): 934-939.

Hermo, L., R. M. Pelletier, et al. (2010). "Surfing the wave, cycle, life history, and genes/proteins expressed by testicular germ cells. Part 1: Background to spermatogenesis, spermatogonia, and spermatocytes." Microscopy Research and Technique **73**(4): 241-278.

Hinton, B. T. and T. G. Cooper (2010). The Epididymis as a Target for Male Contraceptive Development. Fertility Control. U.-F. Habenicht and R. J. Aitken, Springer Berlin Heidelberg. **198:** 117-137.

Hoffer, A. P. (1972). "The fine structure of the ductuli efferentes in mouse and rat. ." Anat. Rec. **172**: 331-332.

Hoffer, A. P. and J. Greenberg (1978). "The structure of the epididymis, efferent ductules and ductus deferens of the guinea pig: a light microscope study. ." Anat. Rec. **190**: 659-678.

Hrabchak, C., H. Henderson, et al. (2007). "A Testis Specific Isoform of Endophilin B1, Endophilin B1t, Interacts Specifically with Protein Phosphatase-1cγ2 in Mouse Testis and Is Abnormally Expressed in PP1cγ Null Mice." Biochemistry **46**(15): 4635-4644.

Hrabchak, C. and S. Varmuza (2004). "Identification of the Spermatogenic Zip Protein Spz1 as a Putative Protein Phosphatase-1 (PP1) Regulatory Protein That Specifically Binds the PP1c2 Splice Variant in Mouse Testis." THE JOURNAL OF BIOLOGICAL CHEMISTRY **279**: 37079-37086.

Hrabchak, C. and S. Varmuza (2004). "Identification of the Spermatogenic Zip Protein Spz1 as a Putative Protein Phosphatase-1 (PP1) Regulatory Protein That Specifically Binds the PP1cγ2 Splice Variant in Mouse Testis." Journal of Biological Chemistry **279**(35): 37079-37086.

Huang, L. J., L. Wang, et al. (1999). "NH2-Terminal targeting motifs direct dual specificity A-kinase-anchoring protein 1 (D-AKAP1) to either mitochondria or endoplasmic reticulum." J Cell Biol **145**(5): 951-959.

Huang, Z., B. Khatra, et al. (2002). "Sperm PP1γ2 Is Regulated by a Homologue of the Yeast Protein Phosphatase Binding Protein sds221." Biology of Reproduction **67**(6): 1936-1942.

Huang, Z., K. Myers, et al. (2004). "Protein 14-3-3ζ Binds to Protein Phosphatase PP1γ2 in Bovine Epididymal Spermatozoa." Biology of Reproduction **71**(1): 177-184.

Huang, Z., P. R. Somanath, et al. (2005). "Changes in Intracellular Distribution and Activity of Protein Phosphatase PP1γ2 and Its Regulating Proteins in Spermatozoa Lacking AKAP4." Biology of Reproduction **72**(2): 384-392.

Hurley, T. D., J. Yang, et al. (2007). "Structural basis for regulation of protein phosphatase 1 by inhibitor-2." J Biol Chem **282**(39): 28874-28883.

Ito, M., T. Nakano, et al. (2004). "Myosin phosphatase: Structure, regulation and function." Molecular and Cellular Biochemistry **259**(1): 197-209.

Ivell, R., S. Danner, et al. (2004). "Post-meiotic gene products as targets for male contraception." Molecular and Cellular Endocrinology **216**(1-2): 65-74.

Jaroszynski, L., J. Zimmer, et al. (2010). "Translational control of the AZFa gene DDX3Y by 5′UTR exon-T extension." International Journal of Andrology: no-no.

Jin, X. P., F. Huang, et al. (2001). "GABA transporter 1 transcriptional starting site exhibiting tissue specific difference." Cell Res **11**(2): 161-163.

Johnson, D. F., G. Moorhead, et al. (1996). "Identification of protein-phosphatase-1-binding domains on the glycogen and myofibrillar targetting subunits." European Journal of Biochemistry **239**(2): 317-325.

Johnson, L. and D. D. Varner (1988). "Effect of daily spermatozoan production but not age on transit time of spermatozoa through the human epididymis." Biology of Reproduction **39**(4): 812-817.

Jurisicova, A., S. Lopes, et al. (1999). "DNA damage in round spermatids of mice with a targeted disruption of the Pp1cγ gene and in testicular biopsies of patients with non-obstructive azoospermia." Molecular Human Reproduction **5**(4): 323-330.

Kao, S.-C., C.-Y. Chen, et al. (2007). "Identification of phostensin, a PP1 F-actin cytoskeleton targeting subunit." Biochemical and Biophysical Research Communications **356**(3): 594-598.

Kawabe, T., A. J. Muslin, et al. (1997). "HOX11 interacts with protein phosphatases PP2A and PP1 and disrupts a G2/M cell-cycle checkpoint." Nature **385**(6615): 454-458.

Kessler, S. P., T. M. Rowe, et al. (2000). "Physiological Non-equivalence of the Two Isoforms of Angiotensin-converting Enzyme." Journal of Biological Chemistry **275**(34): 26259-26264.

Kirchner, J., S. Gross, et al. (2007). "Essential, Overlapping and Redundant Roles of the Drosophila Protein Phosphatase 1{alpha} and 1{beta} Genes." Genetics **176**(1): 273-281.

Koppers, A. J., T. Reddy, et al. (2011). "The role of cysteine-rich secretory proteins in male fertility." Asian Journal of Andrology **13**(111-117).

Koshibu, K., J. Graff, et al. (2009). "Protein Phosphatase 1 Regulates the Histone Code for Long-Term Memory." J. Neurosci. **29**(41): 13079-13089.

Krege, J. H., S. W. M. John, et al. (1995). "Male–female differences in fertility and blood pressure in ACE-deficient mice." Nature **375**(6527): 146-148.

Kwiek, N. C., D. F. Thacker, et al. (2006). "PITK, a PP1 targeting subunit that modulates the phosphorylation of the transcriptional regulator hnRNP K." Cell Signal **18**(10): 1769-1778.

Landsverk, H. B., M. Kirkhus, et al. (2005). "PNUTS enhances in vitro chromosome decondensation in a PP1-dependent manner." Biochemical Journal **390**(3): 709-717.

Larry, J., L. T. Donald, et al. (2008). "Role of Sertoli cell number and function on regulation of spermatogenesis." Animal reproduction science **105**(1): 23-51.

LeBlond, C. and Y. Clermont (1952). "Definition of the stages of the cycle of the seminiferous epithelium in the rat." Ann NY Acad Sci **55**: 548-573.

Lejeune, H., R. Habert, et al. (1998). "Origin, proliferation and differentiation of Leydig cells." J Mol Endocrinol **20**(1): 1-25.

Lesage, B., M. Beullens, et al. (2007). "A complex of catalytically inactive protein phosphatase-1 sandwiched between Sds22 and inhibitor-3." Biochemistry **46**(31): 8909-8919.

Li, L., C. H. Ren, et al. (2003). "Caveolin-1 maintains activated Akt in prostate cancer cells through scaffolding domain binding site interactions with and inhibition of serine/threonine protein phosphatases PP1 and PP2A." Mol Cell Biol **23**(24): 9389-9404.

Li, M., D. L. Satinover, et al. (2007). "Phosphorylation and functions of inhibitor-2 family of proteins." Biochemistry **46**(9): 2380-2389.

Liao, H., Y. Li, et al. (1998). "Protein Phosphatase 1 Is Targeted to Microtubules by the Microtubule-associated Protein Tau." Journal of Biological Chemistry **273**(34): 21901-21908.

Lie, P. P. Y., D. D. Mruk, et al. (2010). "Cytoskeletal dynamics and spermatogenesis." Philosophical Transactions of the Royal Society B: Biological Sciences **365**(1546): 1581-1592.

Lin, C. Y., B. C.-M. Tan, et al. (2010). "Dephosphorylation of Nucleophosmin by PP1{beta} Facilitates pRB Binding and Consequent E2F1-dependent DNA Repair." Mol. Biol. Cell **21**(24): 4409-4417.

Liu, Y., D. M. Virshup, et al. (2002). "Regulation of BRCA1 Phosphorylation by Interaction with Protein Phosphatase 1α." Cancer Research **62**(22): 6357-6361.

Liu, Y., D. M. Virshup, et al. (2002). "Regulation of BRCA1 phosphorylation by interaction with protein phosphatase 1alpha." Cancer Res **62**(22): 6357-6361.

Llorian, M., M. Beullens, et al. (2004). "SIPP1, a novel pre-mRNA splicing factor and interactor of protein phosphatase-1." Biochem J.(Pt 1): . **378**: 229-238.

Lou, Y., W. Xie, et al. (2004). "Nek2A specifies the centrosomal localization of Erk2." Biochemical and Biophysical Research Communications **321**(2): 495-501.

MacMillan, L. B., M. A. Bass, et al. (1999). "Brain Actin-associated Protein Phosphatase 1 Holoenzymes Containing Spinophilin, Neurabin, and Selected Catalytic Subunit Isoforms." Journal of Biological Chemistry **274**(50): 35845-35854.

Maekawa, M., K. Kamimura, et al. (1996). "Peritubular myoid cells in the testis: their structure and function." Arch Histol Cytol. **59(1)**: 1-13.

Margolis, S. S., S. Walsh, et al. (2003). "PP1 control of M phase entry exerted through 14-3-3-regulated Cdc25 dephosphorylation." EMBO J **22**(21): 5734-5745.

Mayhew, T. M. and J. M. Lucocq (2008). "Developments in cell biology for quantitative immunoelectron microscopy based on thin sections: a review." Histochem Cell Biol **130**: 299–313.

McLachlan, R. I., L. O'Donnell, et al. (2002). "Identification of Specific Sites of Hormonal Regulation in Spermatogenesis in Rats, Monkeys, and Man." Recent Prog Horm Res **57**(1): 149-179.

Mishra, S., P. R. Somanath, et al. (2003). "Binding and inactivation of the germ cell-specific protein phosphatase PP1gamma2 by sds22 during epididymal sperm maturation." Biol Reprod **69**(5): 1572-1579.

Morimoto, H., H. Okamura, et al. (2002). "Interaction of Protein Phosphatase 1 Delta with Nucleolin in Human Osteoblastic Cells." Journal of Histochemistry & Cytochemistry **50**(9): 1187-1193.

Nicolaou, P. and E. G. Kranias (2009). "Role of PP1 in the regulation of Ca cycling in cardiac physiology and pathophysiology." Front Biosci **14**: 3571-3585.

Oliver, C. (1994). Fixation and embedding. In: Javois LC editor. Methods in Molecular Biology. Totowa, New Jersey, Humana Press.

Olsen, J. V., B. Blagoev, et al. (2006). "Global, In Vivo, and Site-Specific Phosphorylation Dynamics in Signaling Networks." Cell **127**(3): 635-648.

Olson, G. E., S. K. NagDas, et al. (2002). Structural differentiation of spermatozoa during post-testicular maturation. In The Epididymis: from Molecules To Clinical Practice, . New York, Kluwer Academic/Plenum Publishers.

Oppedisano, L., G. Haines, et al. (2002). "The rate of aneuploidy is altered in spermatids from infertile mice." Human Reproduction **17**(3): 710-717.

Orth, J. M., G. L. Gunsalus, et al. (1988). "Evidence From Sertoli Cell-Depleted Rats Indicates That Spermatid Number in Adults Depends on Numbers of Sertoli Cells Produced During Perinatal Development." Endocrinology **122**(3): 787-794.

Ouimet, C. C., E. F. da Cruz e Silva, et al. (1995). "The alpha and gamma 1 isoforms of protein phosphatase 1 are highly and specifically concentrated in dendritic spines." Proceedings of the National Academy of Sciences of the United States of America **92**(8): 3396-3400.

Parrish, J. R., K. D. Gulyas, et al. (2006). "Yeast two-hybrid contributions to interactome mapping." Curr Opin Biotechnol **17**(4): 387-393.

Pauls, K., R. Metzger, et al. (2003). "Isoforms of angiotensin I-converting enzyme in the development and differentiation of human testis and epididymis." Andrologia **35**(1): 32-43.

Prince, F. P. (1990). "Ultrastructural evidence of mature Leydig cells and Leydig cell regression in the neonatal human testis." The Anatomical Record **228**(4): 405-417.

Publicover, S., C. V. Harper, et al. (2007). "[Ca2+]i signalling in sperm [mdash] making the most of what you've got." Nat Cell Biol **9**(3): 235-242.

Puri, P., K. Myers, et al. (2008). "Proteomic analysis of bovine sperm YWHA binding partners identify proteins involved in signaling and metabolism." Biol Reprod **79**(6): 1183-1191.

Roberts, K. P. (2002). "The Epididymis: From Molecules to Clinical Practice: A Comprehensive Survey of the Efferent Ducts, the Epididymis and Vas Deferens: edited by Bernard Robaire and Barry T. Hinton, 575 pp., with author and subject indices, New York, NY: Kluwer Academic and Plenum Publishers; 2002. ISBN 0-306-46684-8." J Androl **23**(5): 620-.

Ross, M. H. and I. R. Long (1966). "Contractile Cells in Human Seminiferous Tubules." Science **153**(3741): 1271-1273.

Rowley, M., F. Teshima, et al. (1970). "Duration of transit of spermatozoa through the human male ductular system.

." Fertil Steril. **21(5)**: 390-396.

Sambrook, J., Fritsch, E. F., Maniatis, T. (1989). Molecular cloning: a laboratory manual. USA, Cold Spring Harbor Laboratory Press.

Schwarz, H. and H. Hohenberg (2001). Immuno-electron Microscopy, John Wiley & Sons, Ltd.

Shima, H., Y. Hatano, et al. (1993). "Identification of PP1 Catalytic Subunit Isotypes PP1[gamma]1, Pp1[delta] and Pp1[alpha] in Various Rat Tissues." Biochemical and Biophysical Research Communications **192**(3): 1289-1296.

Sobue, K., A. Agarwal-Mawal, et al. (2000). "Interaction of neuronal Cdc2-like protein kinase with microtubule-associated protein tau." J Biol Chem **275**(22): 16673-16680.

Standring, S. (2005). Gray´s Anatomy: The Anatomical Basis of Clinical Practice. Spain, Elsevier Churchill Liningstone.

Steen, R. L., M. Beullens, et al. (2003). "AKAP149 is a novel PP1 specifier required to maintain nuclear envelope integrity in G1 phase." J Cell Sci **116**(Pt 11): 2237-2246.

Stelzer, G. and J. Don (2002). "Atce1: A Novel Mouse Cyclic Adenosine 3',5'-Monophosphate-Responsive Element-Binding Protein-Like Gene Exclusively Expressed in Postmeiotic Spermatids." Endocrinology **143**(5): 1578-1588.

Strack, S., S. Kini, et al. (1999). "Differential cellular and subcellular localization of protein phosphatase 1 isoforms in brain." The Journal of Comparative Neurology **413**(3): 373-384.

Sullivan, R., G. Frenette, et al. (2007). "Epididymosomes are involved in the acquisition of new sperm proteins during epididymal transit." Asian J Androl **9**(4): 483-491.

Svechnikov, K., L. Landreh, et al. (2010). "Origin, Development and Regulation of Human Leydig Cells." Hormone Research in Paediatrics **73**(2): 93-101.

Svenningsson, P., A. Nishi, et al. (2004). "DARPP-32: An Integrator of Neurotransmission." Annual Review of Pharmacology and Toxicology **44**(1): 269-296.

Takayuki, F., T. Kazutoshi, et al. (2001). "Use of stepwise subtraction to comprehensively isolate mouse genes whose transcription is up-regulated during spermiogenesis " EMBO reports: 367–372.

Terrak, M., F. Kerff, et al. (2004). "Structural basis of protein phosphatase 1 regulation." Nature **429**(6993): 780-784.

Terry-Lorenzo, R. T., E. Elliot, et al. (2002). "Neurabins Recruit Protein Phosphatase-1 and Inhibitor-2 to the Actin Cytoskeleton." Journal of Biological Chemistry **277**(48): 46535-46543.

Thimon, V., O. Koukoui, et al. (2007). "Region-specific gene expression profiling along the human epididymis." Molecular Human Reproduction **13**(10): 691-704.

Toole, B. J. and P. T. W. Cohen (2007). "The skeletal muscle-specific glycogen-targeted protein phosphatase 1 plays a major role in the regulation of glycogen metabolism by adrenaline in vivo." Cellular Signalling **19**(5): 1044-1055.

Tran, P., D. Leclerc, et al. (2002). "Multiple transcription start sites and alternative splicing in the methylenetetrahydrofolate reductase gene result in two enzyme isoforms." Mammalian Genome **13**(9): 483-492.

Trinkle-Mulcahy, L., P. Ajuh, et al. (1999). "Nuclear organisation of NIPP1, a regulatory subunit of protein phosphatase 1 that associates with pre-mRNA splicing factors." J Cell Sci **112**(2): 157-168.

Trinkle-Mulcahy, L., J. Andersen, et al. (2006). "Repo-Man recruits PP1γ to chromatin and is essential for cell viability." The Journal of Cell Biology **172**(5): 679-692.

Trinkle-Mulcahy, L., P. D. Andrews, et al. (2003). "Time-lapse Imaging Reveals Dynamic Relocalization of PP1gamma throughout the Mammalian Cell Cycle." Mol. Biol. Cell **14**(1): 107-117.

Trinkle-Mulcahy, L., J. E. Sleeman, et al. (2001). "Dynamic targeting of protein phosphatase 1 within the nuclei of living mammalian cells." J Cell Sci **114**(23): 4219-4228.

Vagnarelli, P., D. F. Hudson, et al. (2006). "Condensin and Repo-Man-PP1 co-operate in the regulation of chromosome architecture during mitosis." Nat Cell Biol **8**(10): 1133-1142.

Varmuza, S., A. Jurisicova, et al. (1999). "Spermiogenesis Is Impaired in Mice Bearing a Targeted Mutation in the Protein Phosphatase 1cg Gene." Developmental Biology **205**: 98-110.

Vernet, P., R. J. Aitken, et al. (2004). "Antioxidant strategies in the epididymis." Molecular and Cellular Endocrinology **216**(1-2): 31-39.

Vijayaraghavan, S., S. A. Goueli, et al. (1997). "Protein Kinase A-anchoring Inhibitor Peptides Arrest Mammalian Sperm Motility." Journal of Biological Chemistry **272**(8): 4747-4752.

Vijayaraghavan, S. and D. D. Hoskins (1986). "Regulation of bovine sperm motility and cyclic adenosine 3',5'-monophosphate by adenosine and its analogues." Biology of Reproduction **34**(3): 468-477.

Vijayaraghavan, S., G. A. Liberty, et al. (1999). "Isolation and molecular characterization of AKAP110, a novel, sperm-specific protein kinase A-anchoring protein." Mol Endocrinol **13**(5): 705-717.

Vijayaraghavan, S., D. T. Stephens, et al. (1996). "Sperm motility development in the epididymis is associated with decreased glycogen synthase kinase-3 and protein phosphatase 1 activity." Biol Reprod **54**(3): 709-718.

Visconti, P. E., L. R. Johnson, et al. (1997). "Regulation, localization, and anchoring of protein kinase A subunits during mouse sperm capacitation." Dev Biol **192**(2): 351-363.

Wakula, P., M. Beullens, et al. (2006). "The translation initiation factor eIF2beta is an interactor of protein phosphatase-1." Biochem J **400**(2): 377-383.

Wang, R., A. Kaul, et al. (2010). "TLRR (lrrc67) interacts with PP1 and is associated with a cytoskeletal complex in the testis." Biology of the Cell **102**(3): 173-189.

Westphal, R. S., S. J. Tavalin, et al. (1999). "Regulation of NMDA receptors by an associated phosphatase-kinase signaling complex." Science **285**(5424): 93-96.

WHO (2010). WHO laboratory manual for the examination and processing of human semen, Department of Reproductive Health and Research.

Wilhelm, D. and P. Koopman (2006). "The makings of maleness: towards an integrated view of male sexual development." Nat Rev Genet **7**(8): 620-631.

Wu, W., J. E. Baxter, et al. (2007). "Alternative splicing controls nuclear translocation of the cell cycle-regulated Nek2 kinase." J Biol Chem **282**(36): 26431-26440.

Wu, W., J. E. Baxter, et al. (2007). "Alternative Splicing Controls Nuclear Translocation of the Cell Cycle-regulated Nek2 Kinase." Journal of Biological Chemistry **282**(36): 26431-26440.

Yang, P., L. Fox, et al. (2000). "Protein phosphatases PP1 and PP2A are located in distinct positions in the Chlamydomonas flagellar axoneme." J Cell Sci **113**(1): 91-102.

Yoshida, S., M. Sukeno, et al. (2007). "A Vasculature-Associated Niche for Undifferentiated Spermatogonia in the Mouse Testis." Science **317**(5845): 1722-1726.

Zhang, J.-S., Q. Liu, et al. (2006). "Genome-wide profiling of segmental-regulated transcriptomes in human epididymis using oligo microarray." Molecular and Cellular Endocrinology **250**(1-2): 169-177.

Zhou, Y., P. Delafontaine, et al. (1995). "Identification of two positive transcriptional elements within the 91-base pair promoter for mouse testis angiotensin converting enzyme (testis ACE)." Dev Genet. **16(2)**: 201-209.

APPENDIX

SOLUTIONS FOR MICROSCOPY

Almost all the reagents used in processing samples for electron and immunoelectron microscopy are potentially hazardous to various degrees.

Citrate buffer	Buffer A: 1mM $C_6H_8O_7H_2O$ Buffer B: 50 mM $C_6H_5Na_3O_72H_2O$ Citrate buffer: 0.15 mM Buffer A, 8.5 mM Buffer B, pH 6.0
Epoxy resin	24 g Agar 100, 16 g DDSA, 10 g MNA, 1.5 g BDMA
Fixation solution A for EM and IEM	0.5% glutaraldehyde, 1% paraformaldehyde, 0.025% picric acid, 0.1 M cacodylate buffer, pH 7.4
Buffer A	0.1 M cacodylate buffer, pH 7.4
Fixation solution B for EM and IEM	0.05% glutaraldehyde, 4% paraformaldehyde, 2% sucrose, 0.1M HEPES, pH 7.4
Buffer B	0.1M HEPES, pH 7.4
Glycine solution	0.05 M glycine in TBS 1x, pH 7.4
IHC blocking solution	4% BSA in TBST 1x, pH 7.4
IEM blocking solution	1% BSA in TBST 1x, pH 7.4
Lead citrate (Reynold's)	0.19 mM lead nitrate, 0.22 mM sodium citrate, shake 30 min, ddH_2O up to 25 ml, pH 10.0
Osmium post-fixation for EM	1-2% aqueous osmium tetroxide
PBS 10x	1.5 M NaCl, 131 mM K_2HPO_4, 50 mM KH_2PO_4, pH 7.4
Rudeberg solution	0.1 g Methylenblue; 0.1 g thionin; 1.42 g $NaHPO_4$; 70 ml dH_2O; 30 ml glycerin solution; Dissolve and filter (0.2 µm filter) the solution
TBS 10x	0.5 M Tris, 1.5 M NaCl, fill up to 1L ddH_2O, pH 7.4
TBST 10x	0.5 M Tris, 1.5 M NaCl, 0.05% Tween 20, fill up to 1L ddH_2O, pH 7.4
Trypsin	0.01% trypsin in TBS 1x
Uranyl acetate	1% uranyl acetate in ddH_2O; prior use centrifuge 15 min
Washing solution for EM and IEM	0.1% BSA in TBST, pH 7.4

ELECTRON MICROSCOPY IMAGES

Figure 28| Resin blocks for EM.

Figure 29| Box to store the nickel grids.

Figure 30| LEO 906 electron microscope.

SOLUTIONS FOR SPERM PROCESSING

HB buffer (1 L)		
Reagent	**Final Concentration**	**Quantity**
1 M Tris pH 7.0	10 mM	10 mL
100 mM EDTA	1 mM	10 mL
100 mM EGTA	1 mM	10 mL
dH_2O	-	970 mL
Adjust pH to 7.0		
HB plus buffer (5 mL)		
Reagent	**Final Concentration**	**Quantity**
HB buffer	-	5mL
200 mM Benzamidine	10mM	250 µL
100mM PMSF in 100% etanol	1mM	50 µL
1,5 mM Pepstatin A	5 µM	16,7 µL
10,8 mM Leupeptin	2 µM	0.9 µL
0,169 mM Aprotitin	1.5 µM	44.4 µL
100 mM EGTA	1 mM	50.5 µL

IMPROVED NEUBAUER HAEMOCYTOMETER

The improved Neubauer haemocytometer has two separate counting chambers, each of which has a microscopic 3 mm × 3 mm pattern of gridlines etched on the glass surface.

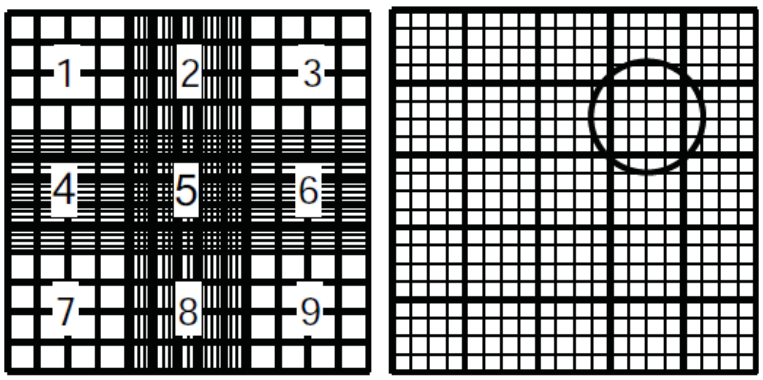

Figure 31| The improved Neubauer haemocytometer. Left panel: all nine grids in one chamber of the haemocytometer; With a depth of 100 µm, each grid holds 100 nl. Four of these grids (1, 3, 7 and 9) contain four rows of four squares, each holding 6.25 nl; two grids (2 and 8) contain four rows of fi ve squares, each of 5 nl; two grids (4 and 6) contain five rows of four squares, each of 5 nl; and the central grid (number 5) contains five rows of five squares, each of 4 nl (Right panel).

SOLUTIONS FOR WESTERN BLOT

LGB (Lower Gel Buffer)	To 900 ml of deionized H_2O add: Tris 181.65 g SDS 4 g Mix until the solutes have dissolved. Adjust the pH to 8.9 and adjust the volume to 1L with deionized H_2O
UGB (Upper Gel Buffer)	To 900 ml of deionized H_2O add: Tris 75.69 g Mix until the solute has dissolved. Adjust the pH to 6.8 and adjust the volume to 1L with deionized H_2O
30%Acrylamide/ 0.8%Bisacrylamide	To 70 ml of deionized H_2O add: Acrylamide 29.2 g Bisacrylamide 0.8 g Mix until the solutes have dissolved. Adjust the volume to 100 mL with deionized H_2O. Filter through a 0.2 μm filter and store at 4 °C
10% APS (ammonium persulfate)	In 10 ml of deionized H_2O dissolve 1 g of APS
10% SDS (sodium dodecilsulfate)	In 10 ml of deionized H_2O dissolve 1 g of SDS
4x Loading gel buffer	1 M Tris solution (pH 6.8) 2.5 ml (250 mM) SDS 0.8 g (0.8%) Glycerol 4 ml (40%) β-Mercaptoethanol 2 ml (2%) Bromophenol blue 1 mg (0.01 %) Adjust the volume to 10 ml with deionized H_2O. Store in darkness at RT
1 M Tris (pH 6.8) solution	To 150 ml of deionized H_2O add: Tris base 30.3 g Adjust the pH to 6.8 and adjust the final volume to 250 ml
10x Running buffer	Tris 30.3 g (250 mM) Glycine 144.2 g (2.5 M) SDS 10 g (1%) Dissolve in deionized H_2O, adjust the pH to 8.3 and adjust the volume to 1L

10x Transfer buffer	Tris 3.03 g (25 mM) Glycine 14.41 g (192 mM) Mix until solutes dissolution. Adjust the pH to 8.3 with HCl and adjust the volume to 800 ml with deionized H_2O. Just prior to use add 200 ml of methanol (20%)
10x TBS (Tris buffered saline)	Tris 12.11 g (10 mM) NaCl 87.66 g (150 mM) Adjust the pH to 8.0 with HCl and adjust the volume to 1 L with deionized H_2O
10x TBST (TBS + Tween)	Tris 12.11 g (10 mM) NaCl 87.66 g (150 mM) Tween 20 5 ml (0.05%) Adjust the pH to 8.0 with HCl and adjust the volume to 1 L with deionized H_2O
Developer Solution	GBX developer 220 ml Adjust the volume to 1 L with deionized H_2O
Fixation Solution	GBX fixer 220 ml Adjust the volume to 1 L with deionized H_2O